Carbon dioxide cycling and implications for climate on ancient Earth

Norman H. Sleep

Department of Geophysics, Stanford University, Stanford, California

Kevin Zahnle

NASA Ames Research Center, Mountain View, California

Abstract. The crustal Urey cycle of CO_2 involving silicate weathering and metamorphism acts as a dynamic climate buffer. In this cycle, warmer temperatures speed silicate weathering and carbonate formation, reducing atmospheric CO_2 and thereby inducing global cooling. Over long periods of time, cycling of CO_2 into and out of the mantle also dynamically buffers CO_2. In the mantle cycle, CO_2 is outgassed at ridge axes and island arcs, while subduction of carbonatized oceanic basalt and pelagic sediments returns CO_2 to the mantle. Negative feedback is provided because the amount of basalt carbonatization depends on CO_2 in seawater and therefore on CO_2 in the air. On the early Earth, processes involving tectonics were more vigorous than at present, and the dynamic mantle buffer dominated over the crustal one. The mantle cycle would have maintained atmospheric and oceanic CO_2 reservoirs at levels where the climate was cold in the Archean unless another greenhouse gas was important. Reaction of CO_2 with impact ejecta and its eventual subduction produce even lower levels of atmospheric CO_2 and small crustal carbonate reservoirs in the Hadean. Despite its name, the Hadean climate would have been freezing unless tempered by other greenhouse gases.

1. Introduction

Evidence for relatively mild climates on ancient Earth has been a puzzle in light of the faint early Sun. The geologic evidence, although far from conclusive, would appear to indicate that the surface was, if anything, warmer at 3-4 Ga than it is now, but the astrophysical argument that the Sun ought to have brightened ~30% since it reached the main sequence is hard to refute. There results a paradox between the icehouse we expect and the greenhouse we think we see [*Ringwood*, 1961; *Sagan and Mullen*, 1972; *Kiehl and Dickinson*, 1987; *Pavlov et al.*, 2000]. The usual fix has been to posit massive CO_2 atmospheres [*Owen et al.*, 1979; *Kasting*, 1993], although reduced gases (e.g., NH3 or CH4) have had their partisans [*Sagan and Mullen*, 1972]. Evidence against siderite in paleosols dated at 2.2-2.75 Ga has been used to set a rough upper limit of 30 present atmospheric levels (PAL, where one PAL is 300 ppm) on $pCO2$ at that time [*Rye et al.*, 1995]. This is an order of magnitude short of what is needed to defeat the faint Sun [*Rye et al.*, 1995]. Evidence for a few extremely cold episodes ("snowball Earths" [e.g., *Hoffman and Schrag*, 2000]) ca. 2.3 Ga and 0.6-0.8 Ga indicates that $pCO2$ was not always large enough to keep things warm and thereby casts a little more doubt on the hypothesis that CO_2 was the only important greenhouse gas on ancient Earth. We present here an independent argument, based on CO_2 fluxes in to and out of the mantle, that weighs against high pCO_2 on early Earth that applies most strongly to the Archean and the Hadean eras.

We begin by considering the fate of the vast amount of terrestrial CO_2 that is not in the atmosphere. Roughly 6×10^{21} mol

of CO_2 are currently in the crust, and a comparable or larger amount is in the mantle [e.g., *Zhang and Zindler*, 1993]. The current CO_2 mantle outgassing rate, $\sim2.5\times10^{12}$ moles yr^{1} [*Zhang and Zindler*, 1993], is fast enough to double the surface carbonate inventory in 2.4 billion years. The mantle connection would have been stronger during the Archean. To first approximation, under plate tectonics, ocean crust is recycled as the square of the heat flow. On early Earth, with a geothermal source 2-3 times that of today, ocean crust would have been created and subducted 4-9 times faster than today. Outgassing increases proportionately, so that the timescale for doubling crustal carbonate drops to 300-700 Ma. Evidently, the mantle cannot be neglected on Earth's longest timescales. In particular, ingassing is needed to close the mantle cycle. Possibilities include subduction of carbonates directly deposited on the ocean floor (pelagic carbonates), subduction of continental carbonates that are scraped off and dragged down, and subduction of carbonates formed by seawater alteration of the oceanic basalt itself. The latter, in particular, depends on the amount of free CO_2 in the ocean and hence can act as a buffer on atmospheric CO_2 levels.

Our focus in this paper is on the mantle reservoir and the exchange between surface reservoirs and the mantle, using the language and concepts of plate tectonics to extrapolate the CO_2 cycle into the past. The first step is to construct a specific, albeit much simplified, model of the modern CO_2 cycle. The Earth's CO_2 cycle is complicated and not fully understood. For purposes of presentation, we organize our reservoirs and fluxes following *Tajika and Matsui* [1992]. We use arc fluxes modified from *Plank and Langmuir* [1998] and *Sano and Williams* [1996] and ridge fluxes from *Zhang and Zindler* [1993]. We will then accelerate the cycle into the Archean, taking into account the greater influence of the mantle and the diminished influence of the continents. Finally, we will consider the effects of abundant impact ejecta on Hadean cycles.

We will generally neglect the sometimes different behavior of reduced carbon in compiling our estimates, as terms involving reduced C are relatively small and the complications and uncertainties introduced by modeling of the oxygen cycle are relatively large. This precludes our using carbon isotopes to constrain our models.

2. Current Carbonate Cycle

On geologic timescales, CO_2 cycles between rocks, often by way of the ocean and atmosphere. These refractory reservoirs include carbon in the mantle, carbon in continental carbonates, carbon in reduced form mostly in continental shales, and carbon (mostly carbonate) in or on the seafloor. The small volatile reservoir (ocean plus atmosphere) recycles through carbonate rock in a hundred thousand to a million years. Over longer periods, free CO_2 is dynamically controlled by processes that form carbonates at low temperatures and processes that decompose carbonates at high temperatures by (Urey) reactions of the form

$$CO_2 + CaSiO_3 \Leftrightarrow SiO_2 + CaCO_3. \tag{1}$$
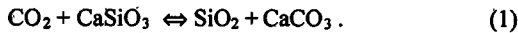
Magnesium and, under reducing conditions, iron carbonates can form by analogous reactions. The continental part of this cycle has been extensively studied [e.g., *Walker*, 1977; *Holland*, 1978, 1984; *Franck et al.*, 1999]. Weathering of rocks on land dissolves carbonates and releases Ca^{2+} from silicates. Both the

dissolved carbonate and the Ca^{2+} are carried by rivers to the oceans, where the Ca^{2+} reacts to form $CaCO_3$. Reaction (1) is reversed when carbonates are metamorphosed deep in the crust. Carbonate weathering,

$$H_2O + CO_2 + CaCO_3 \Leftrightarrow Ca^{++} + 2HCO_3^- \tag{2}$$

has no direct net effect on carbonate reservoirs on timescales longer than a few thousand years, but silicate weathering, by removing free CO_2 from the atmosphere-ocean system, acts to buffer surface temperatures because the weathering rates increase with temperature and temperature increases with atmospheric CO_2 [*Walker et al.*, 1981; *Lasaga et al.*, 1985].

2.1. Fluxes and Reservoirs

Figure 1 represents our summary of the modern CO_2 cycle. We consider five significant reservoirs: the atmosphere, R_{atm}; free carbonate in the ocean, R_{ocean}; carbonates lying upon (R_{pel}) or veined within (R_{bas}) oceanic basalt; carbonates on continental platforms, R_{con}; and CO_2 in the mantle, R_{man}.

The atmosphere and ocean are linked by the effective solubility of CO_2. There are currently 6.2×10^{16} mol of CO_2 in the atmosphere and 3.3×10^{18} mol in the oceans; the ratio is 54:1. These reservoirs are tightly coupled on geological timescales, so that the air is refreshed in a thousand years. In compiling budgets we will treat R_{atm} and R_{ocean} as a single reservoir, denoted R_{oc}, with a current size of $\sim 3.3 \times 10^{18}$ mol.

Now

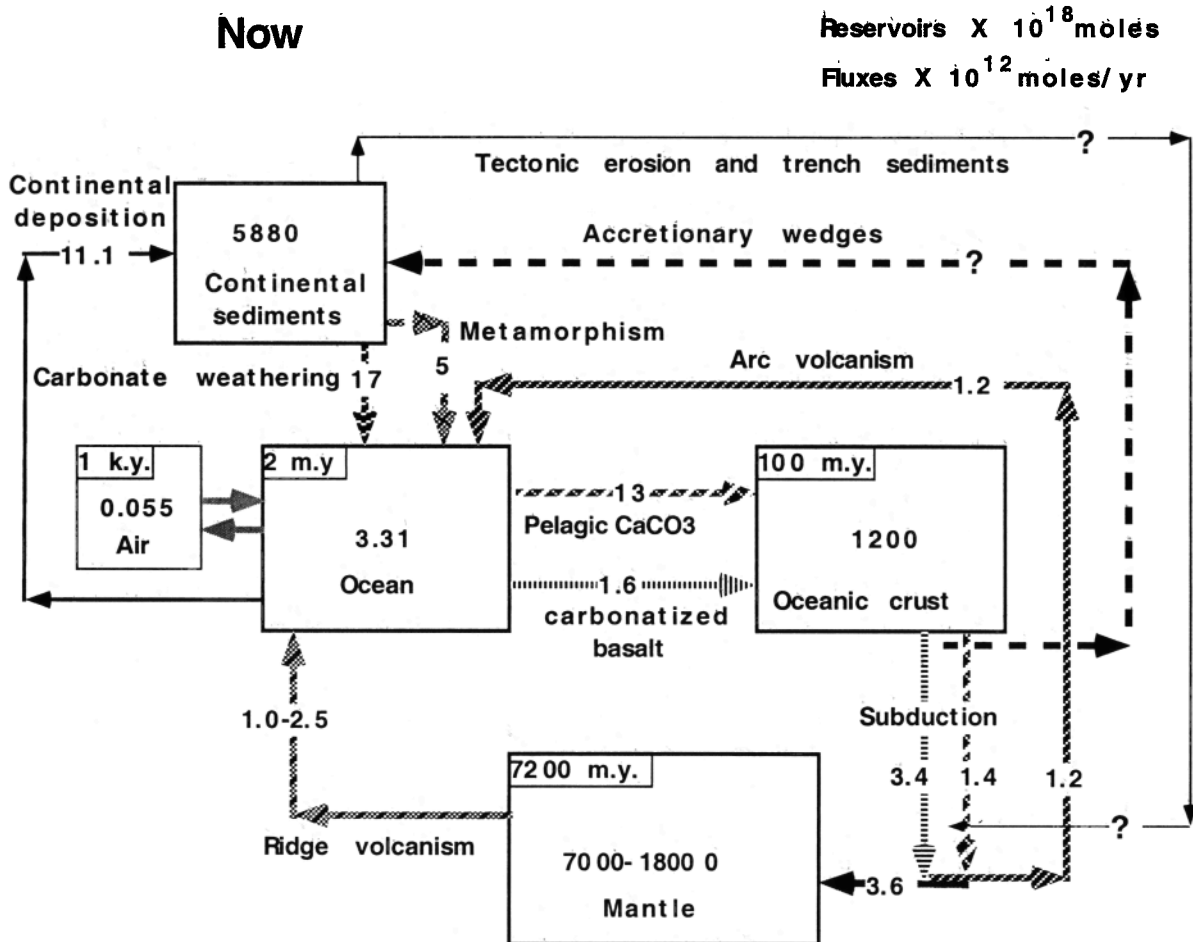Reservoirs X 10^{18} moles

Fluxes X 10^{12} moles/yr

Figure 1. The modern CO_2 cycle, shown with reservoirs (boxes) and fluxes (arrows). The current residence times are shown in the corners of the reservoirs for which they can be usefully defined.

The reservoirs are linked by fluxes that are labeled by process in Figure 1. In no particular order, these are carbonate weathering F_{CO_3w} and its reverse, carbonate deposition on continental platforms F_{ppt}; silicate weathering F_{SiO_2w} and its reverse, carbonate metamorphism F_{meta}; pelagic carbonate deposition on the ocean crust F_{pel}; hydrothermal carbonatization of the ocean crust F_{hydro}; subduction F_{sub}; arc volcanism F_{arc}; tectonic erosion F_{tect} (by which we denote the transfer of epicontinental carbonate to the subducting slab); "off-scraping" F_{scrape} of carbonates from the ocean floor to the continental margins of continents, effectively the reverse of F_{tect}; and outgassing from the midocean ridges F_{ridge}. For the Hadean we add the carbonatization of impact ejecta, F_{ej}.

It is useful to write explicitly the relationships depicted in Figure 1 in the form of equations. The budget for R_{oc} as it appears in Figure 1 can be written as

$$\frac{\partial R_{oc}}{\partial t} = F_{meta} + F_{ridge} + F_{arc} + F_{CO_3w}$$
$$- F_{ppt} - F_{pel} - F_{SiO_2w} - F_{hydro} - F_{ej} \quad . \quad (3)$$

Sources are the metamorphic flux, outgassing at the midocean ridge outgassing associated with arc volcanoes, and carbonate weathering. Sinks are carbonate deposition on continental platforms, pelagic carbonate deposition on oceanic crust, silicate weathering on continents, carbonatization of oceanic crust in warm hydrothermal systems, and carbonatization of impact ejecta, respectively.

The carbonate budget for the oceanic crust $R_{bas}+R_{pel}$ can be written as

$$\frac{\partial \left(R_{bas} + R_{pel} \right)}{\partial t} = F_{pel} + F_{tect} + F_{hydro} + F_{ej} - F_{sub} - F_{scrape} \quad , \quad (4)$$

where for bookkeeping purposes we define tectonic erosion to mean adding carbonate to the oceanic crust and offscraping to mean removing it before the crust is subducted (Figure 2). Continentally derived trench sediments have essentially the same effect as tectonic erosion in adding carbonate to the subducting oceanic crust.

Pelagic carbonates, tectonic erosion, and carbonatization add to the inventory of carbonate on or in the ocean crust. Losses are
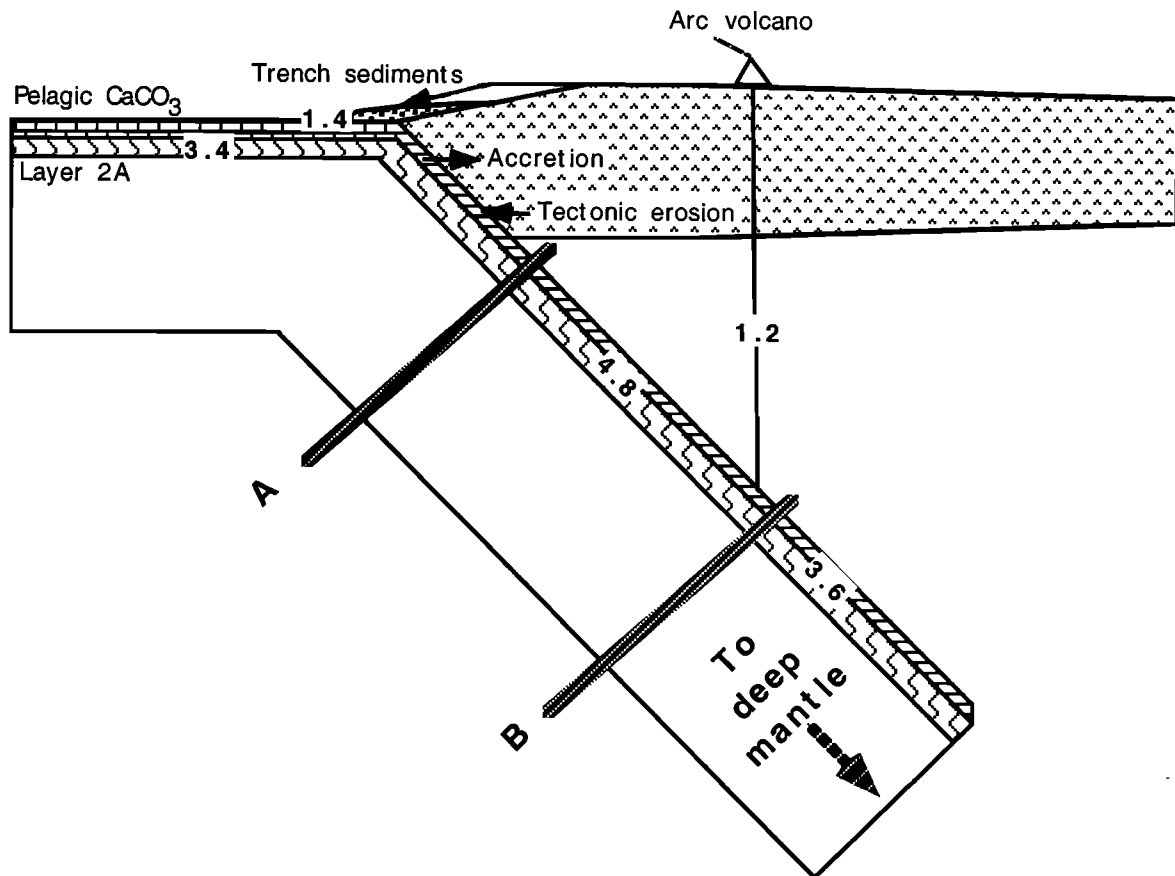
Figure 2. Number representing global fluxes (in units of tmol yr^{-1}), shown superposed on a schematic model of a subduction zone. Pelagic carbonates and carbonatized basalt in oceanic crustal layer 2A (hatched) enter the subduction zone at rates 1.4×10^{12} and 3.4×10^{12} mole yr^{-1}, respectively. Unknown amounts of this material are scraped off and accreted by the continent. Trench sediments and tectonic erosion from the continent add a comparable, albeit also unknown, amount of CO_2 to the slab. For bookkeeping purposes this material is considered to be subducted once it passes beneath the crust of the arc (line A) and to be deeply subducted once it passes beneath the melting region of the arc (line B). Arc volcanoes remove 1.2×10^{12} mol yr^{-1} before the slab reaches the mantle.

subduction and "off-scraping." The former is proportional to R_{bas}, and both are inversely proportional to the lifetime of the oceanic crust. The relative importance of subduction and offscraping depends on whether the carbonate sits on or within the oceanic crust. Pelagic carbonates will be more easily scraped off than would carbonatized basalt. R_{pel} is currently growing because of the geologically recent advent of pelagic carbonates (see section 2.2.1).

The continental and mantle budgets are written as:

$$\frac{\partial R_{con}}{\partial t} = F_{SiO_2w} + F_{ppt} + F_{scrape} - F_{CO_3w} - F_{meta} - F_{tect} , \quad (5)$$

$$\frac{\partial R_{man}}{\partial t} = C_{deep}F_{sub} - F_{ridge} , \quad (6)$$

respectively. Both reservoirs are large. Representative estimates are $R_{con}= 6 \times 10^{21}$ mol and $R_{man}=7$-18×10^{21} mol. Estimates of the mantle reservoir are based on the current ridge outgassing flux, which is constrained only to within a relative factor of a few. At present, R_{con} should be slowly shrinking due to pelagic carbonate deposition. Only the fraction C_{deep} of the total subduction flux F_{sub} reaches the deep mantle, and the balance $(1-C_{deep})F_{sub}=F_{arc}$ comes out through arc volcanoes.

2.2. Simplified Cycle

Although it is not difficult to formally solve the system (3)-(6) using modern computational engines, each process must be assigned a current value and an uncertain history. Mostly, these are at best poorly known and poorly constrained, a recipe almost guaranteed to generate obscure results unless simpler cases are discussed first. A better approach is to simplify the system to the point where relationships are clear and adjustable parameters are reduced to a minimum.

The largest fluxes in (3)-(6) are those associated with carbonate weathering, (2), which consumes and redeposits carbonates at a rate of ~1.7×10^{13} mol yr^{-1}; the associated timescales for recycling the continental carbonates and for recycling free oceanic carbonate are 3.5×10^8 and 2×10^5 years, respectively. It can be argued that carbonate weathering is ignorable because an equivalent amount of carbonate is promptly deposited elsewhere. That is, because carbonate weathering produces both the anion and the cation (e.g., Ca^{+2}), carbonate weathering serves merely to move calcium carbonate from place to place with no change in R_{oc} and no net effect on the overall carbonate budget ($F_{CO3w}=F_{ppt}$). The latter, at least, is not entirely true. At present, carbonate weathering and pelagic deposition are moving carbonate from the continents to the seafloor, so that $F_{CO3w}=F_{ppt}+F_{pel}$. Thus carbonate weathering currently acts as a net sink on continental carbonate, and to the extent that pelagic carbonate is or will be subducted, it will constitute a net loss of crustal carbonate.

2.2.1. Pelagic carbonates.
Pelagic carbonates are an example of transients associated with the finite time for oceanic crust to reach subduction zones. Pelagic carbonates accumulate where the $CaCO_3$ shells made by planktonic organisms fail to dissolve before they reach the ocean floor. In deep water below the carbonate compensation depth, such shells redissolve. However, moderately deep waters, such as near mid-oceanic ridges, are now shallower than the carbonate compensation depth. Shells that sink in these places accumulate and will be carried eventually into subduction zones. There some of the carbonate is scraped off to form accretionary wedges, and some is subducted; of the latter, a fraction is diverted through island arc volcanoes, and the rest

descends to the mantle. Such planktonic organisms precipitated insignificant amounts of carbonate before the middle of the Mesozoic [Sibley and Vogel, 1976], and little pelagic $CaCO_3$ is now being subducted compared to the amount being deposited on the seafloor [Plank and Langmuir, 1998]. Direct constraints on the amount of carbonate scraped off have not been compiled, in part because many exposed wedges are too old to have contained much pelagic carbonate. When globally extrapolated, the Plank and Langmuir [1998] current subduction flux of pelagic CO_2 is 1.4×10^{12} mol yr^{-1}. This is much smaller than the pelagic flux of CO_2 to the ocean floor, 13×10^{12} mol yr^{-1} [Goddéris and François, 1995]. When extrapolating the CO_2 cycle into the deep past, we set F_{pel} to zero.

Significant amounts of continentally derived sediments and crust tectonically eroded by the slab are also subducted. We have lumped these together as F_{tect} Neither organic carbon nor tectonically eroded carbonate are included by Plank and Langmuir's [1998] flux. We assume that together these are of comparable magnitude and opposite sign to the shallow offscraping of sediments. In other words, we take $F_{tect}=F_{scrape}$ and thus render both negligible. It is geologically too soon to tell whether pelagic carbonates will be mostly subducted or mostly scraped off. For this reason, we make no attempt to carry our calculations into the future.

2.2.2. Balanced cycle.
If we take $F_{CO3w}= F_{ppt} + F_{pel}$ and thus assume that carbonate weathering has no effects on R_{oc} other than those associated with changes in the total inventory of crustal carbonate, (3) reduces to an implicit equation for the steady state value of R_{oc}:

$$F_{SiO_2w} + F_{hydro} + F_{ej} = F_{meta} + F_{ridge} + F_{arc} . \quad (7)$$

In (7), the terms on the left-hand side are all monotonically increasing functions of R_{oc}. In addition, silicate weathering rates increase with temperature, which in turn is a function of pCO_2 and therefore of R_{oc}. The terms on the right-hand side are independent of R_{oc}. We will solve this implicit equation for pCO_2 below.

As already noted, silicate weathering and carbonate metamorphism (1) is more important than carbonate weathering (2) because it separates cations from anions. It is interesting because it can act as the Earth's thermostat [Walker et al., 1981]. The combined arc and metamorphic fluxes, estimated at 6 or 6.8×10^{12} mol yr^{-1} [Brantley and Koepenick, 1995, Goddéris and François, 1995], imply that at current rates the continental carbonate inventory is recycled over 800-1000 million years.

It is usually assumed that silicate weathering and metamorphism balance over timescales of hundreds of million years. We review this more familiar case, in which fluxes in and out of the mantle are ignored, to establish context. Silicate weathering is a strong function $f(T)$ of temperature T and (probably) a weak function of pCO_2. For simplicity, we follow Walker et al. [1981] and use

$$F_{SiO_3w} = C_{SiO_3w}pCO_2^{\beta} \exp\left[(T-T_0)/B\right]$$

$$= C_{SiO_3w}pCO_2^{0.3} \exp\left[(T-T_0)/13.7\right], \quad (8a)$$

where $B = 13.7$ and $\beta \approx 0.3$ are the feedback parameters suggested by Walker et al. [1981] and C_{SiO2w} and T_0 are calibration constants. Berner [1994] uses more complicated expressions for silicate weathering that explicitly include topography, runoff, vegetation, and climate feedback. When cast in the form of (8a), Berner's choices are equivalent to taking $B=11.1$ and $\beta = 0.5$, the latter parameter pertinent to Earth

before the advent of vascular land plants. During more recent times, Berner regards silicate weathering as dependent on elevated concentrations of CO_2 in the soil, occurring some 3-10 times faster than weathering without roots [Berner, 1997], but as nearly independent of pCO_2 (roughly equivalent to $\beta \approx 0.14$).

We assume that the metamorphic flux is proportional to the size of the continental reservoir. That is, we take $F_{meta}=R_{con}/\tau_{meta}$, where τ_{meta} is the timescale over which continental carbonate is metamorphosed. Intuitively, one might expect the rate of carbonate metamorphism to scale to the rate at which oceanic crust is recycled by plate tectonics, which in turn, is proportional to the global heat flow squared. Alternatively, metamorphic flux might be proportional to the geothermal gradient, which scales linearly with heat flow. We parameterize this inference by making the rate of carbonate metamorphism proportional to the global heat flow Q to some power $1 < a < 2$. Equation (8a) then can be solved by equating the metamorphism and the silicate weathering fluxes

$$pCO_2^\beta = \frac{F_{meta}}{C_{SiO_2,w}f(T)} \approx \frac{R_{con}/\tau_{meta}}{C_{SiO_2,w}f(T)} \propto \frac{Q^a R_{con}}{f(T)} \qquad (8b)$$

Because the weathering rate is a strong function of surface temperature and a weak function of pCO_2, (8b) describes a strong long-term negative feedback that can regulate pCO_2 and stabilize the surface temperature despite considerable change in solar luminosity.

We can illustrate how the Urey cycle works by using Caldeira and Kasting's [1992] parameterization of the CO_2/water vapor greenhouse effect with an albedo of 31% (so as to reproduce current pCO_2 and T_0) and Walker et al.'s [1981] weathering rates. Studies of paleosols constrain pCO_2 over the last 400 Ma to a range of somewhat less than 1 PAL to 10 PAL [Ekart et al., 1999]. These intermediate term variations are presumably associated with vagaries of plate tectonics on metamorphism and with vagaries of sea level and continent distribution on climate and weathering. To calibrate silicate weathering we assume long-

term average pCO_2 levels of 3.0 PAL and $T_0 = 290$ K. For simplicity, we take global heat flow Q to decline as $(1 - t/4.5)^{0.7}$ and solar luminosity to vary as $L=L_0(1-0.07)t$, where time t is measured backward from the present in billions of years. The heat flow function is arbitrary, but the initial singularity at 4.5 Ga is integrable. Temperature and pCO_2 histories for $a=1$ are shown in Figures 3a and 3b. The silicate weathering exponent is varied between $\beta \approx 0.3$ and $\beta \approx 1$. Constant pCO_2 is shown for comparison. Figures 3a and 3b illustrate that the silicate weathering buffer yields clement ancient climates only if silicate weathering is a weak function of pCO_2. Indeed, the only way this cycle can truly maintain clement surface temperatures is if silicate weathering is nearly independent of pCO_2.

We have not addressed what happens when the predicted global temperature approaches or falls below the freezing point of water. Global glaciation and oceanic ice cover are expected. Such episodes have been inferred from the geological record [Hoffman and Schrag, 2000]. We have not included the effect of ice cover on albedo, which tends to further cool the climate. This difficulty is serious for the balanced cycles in Figures 3a and 3b, which are given mainly for comparison with more complex calculations. The problem is minor for calculations of pCO_2 that involve mantle cycles in sections 2.3 and 3. Our weathering parameterization then suffices by giving sluggish weathering at low temperatures, even though it does not explicitly include glacial processes. That is, during these cold epochs our models with mantle cycles have weathering essentially turned off to the point that its precise value and the precise computed temperature do not matter. Our mantle cycle calculations require only that ice cover does not greatly retard CO_2 equilibration between the ocean and the atmosphere. We address this snowball Earth issue in section 3.2.5.

2.2.3. Weathering kinetics. The matter of reaction kinetics deserves some discussion, as β is the most important ill-constrained parameter in the continental carbonate cycle. If the CO_2 concentration is high, weathering will be limited by diffusion
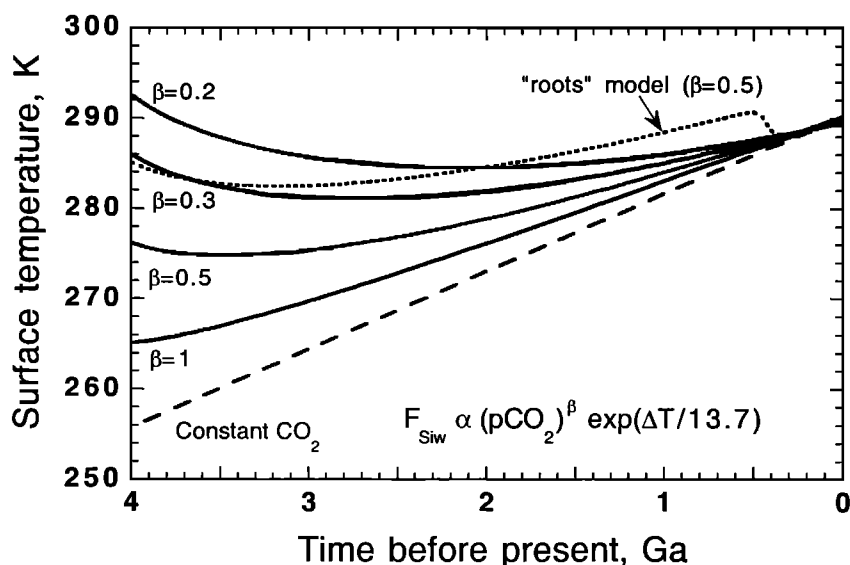
Figure 3a. Global average surface temperatures we predict if the Urey cycle were the only buffer against changing solar luminosity. That is, this model considers only the cycling of CO_2 between crustal reservoirs. The crustal inventory as a whole is constant. The curves are labeled by the weathering parameter β (Equation (8a); see text for details). The "roots" model allows for a change in weathering efficiency beginning with the advent of vascular land plants. Note that ancient climates would be cool.
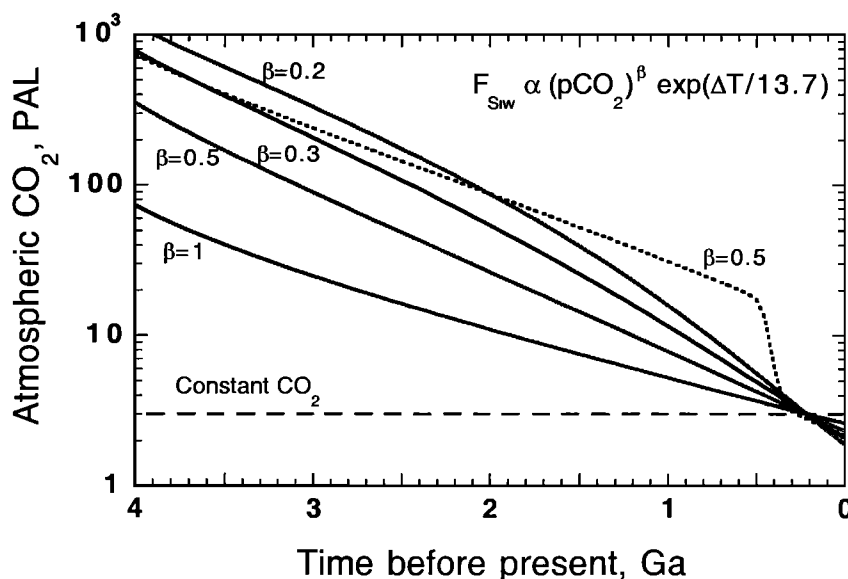
Figure 3b. Atmospheric CO_2 if the Urey cycle were the only buffer against changing solar luminosity. One PAL indicates one "present atmospheric level" of 300 ppm. The curves are labeled by the weathering parameter β. The roots model allows for a change in weathering efficiency beginning with the advent of vascular land plants.

of CO_2 into the rock. For a half-space of constant permeability the reaction rate would go as $pCO_2^{0.5}$. If, instead, we posit a scale-free distribution of fragments of different size, where the cumulative number N of fragments greater than mass m is proportional to $m^{-\gamma}$ (i.e., $N(>m) \propto m^{-\gamma}$), the smaller fragments react fully, while reactions on the surface of the larger fragments form rinds. Carbonate weathering of impermeable grains is said to proceed linearly with time ([*Crovisier et al.*, 1987]; see detailed discussion in section 3.2.2 on ejecta). For this case the reaction rate goes as $pCO_2^{3(1-\gamma)}$ for $2/3 < \gamma < 1$ (the reasonable range for unsorted collisional debris) and linearly as pCO_2 for $\gamma < 2/3$ (i.e., weathering mostly of large blocks); we recover $\beta \approx 0.3$ for $\gamma = 0.9$, which seems a reasonable result for experiments that measure reaction rates of ground-up rock with a superabundance of CO_2 [cf. *Walker et al.*, 1981]. Alternatively, if the substrate is especially finely ground so that $\gamma \geq 1$ or clusters about a preferred size (e.g., Gaussian or lognormal distributions) that is small enough to be fully consumed, the effective dependence of the reaction rate on pCO_2 can be negligible ($\beta = 0$). Finally, if reactable cations are more abundant than CO_2 in the easily permeated material, the reaction rate will go linearly as pCO_2, so that $\beta = 1$. *Berner* [1991, 1994] presents similar discussions and reaches the similar conclusion that $0.25 < \beta < 1$. We will return to the issue of kinetics in the context of carbonatization of oceanic basalt and ejecta in section 3.2.2.

2.2.4. Buffered climate. Two observations pertinent to any successful CO_2 climate buffer are (1) that it takes a lot of CO_2 to maintain clement climates and (2) the predicted climates are not necessarily all that clement. They are markedly cooler than the modern climate through most of the Precambrian and, as such, conflict with the evidence. An additional effect is required, perhaps land plants speeding CO_2 weathering in the Phanerozoic [*Berner*, 1997] or a marked lack of continents in the Precambrian. The need for a lot of CO_2 (e.g., 100-1000 PAL) in the Archean also implies that the ancient oceans must have been much depleted in Ca^{+2} to maintain the present level of supersaturation.

The resulting CO_2-rich, Ca-poor seawater would have been much more effective than modern waters at leaching Ca from basalts and much more prone to carbonatize basalts in situ. Extreme Ca depletion of ancient seawaters would seem to be inconsistent with evidence for evaporitic gypsum [*Buick and Dunlop*, 1990]. Again, the magnitude of the inconsistency can be lessened by a change in weathering style wrought by the advent of land plants.

To quantify the possible effect of plant roots, we compute "roots" models (shown by dotted curves on Figures 3a and 3b) inspired by *Berner* [1994, 1997]. In these models we reduce the weathering rate before the advent of roots to 30% of the current rate. For consistency with *Berner* we use $\beta = 0.5$; for consistency with *Walker et al.* [1981] we also use $\beta \approx 0.3$. The rooted models are very warm at the end of the Precambrian [cf. *Berner* 1997], which may make them an ill match for the climate of the time.

We continue with the mass balance for the crustal carbon reservoir in (5) by considering the case when only silicate weathering and metamorphism are important. That is, we again assume that carbonate weathering has no-long term effect other than to move carbonates from platform to pelagic sediment deposits, $F_{CO3w} = F_{ppt} + F_{pel}$. We effectively ignore off-scraping and tectonic erosion by letting $F_{scrape} = F_{tect}$. Equation (5) then reduces to

$$\frac{dR_{con}}{dt} = F_{SiO_3w} - \frac{R_{con}}{\tau_{meta}} . \qquad (9)$$

This equation, however, is misleading if the mantle processes matter. For example, if the hydrothermal sink in (7) is important, pCO_2 drops below the value that would be set by the crustal thermostat. This decreases silicate weathering while not directly effecting metamorphism, so that the metamorphic flux exceeds the silicate weathering flux, and therefore R_{con} must decrease with time. It is unclear that this situation occurred as the Hadean or Archean Earth would have needed large continental platforms on which to store a bigger R_{con}.

Another perspective on the evolution of R_{con} is to see it instead through the eye of the cation: as a net buildup of Ca^{+2} on continents. Calcium is the only major cation that is markedly overabundant in sedimentary rocks compared to its abundance in the igneous rocks from which sediments were presumably derived [Garrels and Mackenzie, 1971]. Garrels and Mackenzie estimate that there are actually $\sim 2.4 \times 10^{24}$ g of Ca in sediments versus $\sim 9.6 \times 10^{23}$ g that would be expected. The difference, $\sim 3.6 \times 10^{21}$ mol, is comparable to R_{con}. That is, the excess calcium is mostly in carbonate, so that the creation of a large crustal reservoir of carbonate is closely linked to the segregation of calcium. Silicate weathering cannot do this directly because both product and substrate remain on the continent. A process that segregates Ca^{+2} is required. One possibility is that calcium-depleted sediments (e.g., clays) got preferentially subducted [Sibley and Vogel, 1976]. Another would be a net leaching of Ca^{+2} from oceanic basalts or impact ejecta to be precipitated later in shallow seas over continental platforms [Wolery and Sleep, 1988]. The former can be treated formally as an imbalance between off-scraping and tectonic erosion, so that $F_{scrape} > F_{tect}$. The latter can be viewed as an imbalance in the carbonate weathering cycle, in that $F_{ppt} > F_{CO2w} - F_{pel}$. The magnitude of the imbalance corresponds to a net flux of Ca (or CO_2) into continental reservoirs of the order of 2×10^{12} mol yr^{-1} if, say R_{con}, grew at a uniform rate over 2 billion years. The imbalance is thus likely to be significantly smaller than the carbonate weathering and precipitation fluxes themselves, which are closer to $\sim 2 \times 10^{13}$ mol yr^{-1}.

2.3. Mantle Cycles

Both island arcs and ridge axes are heavily involved in the global CO_2 cycle. Offsetting sources and sinks occur at both these plate environments. The magnitude of the fluxes is uncertain but well enough constrained to permit quantification.

2.3.1. Arc volcanism. Arc volcanoes provide a quick return of subducted carbonate to the surface (Figure 2). Sano and Williams [1996] used He/C, carbon isotope ratios, and the assumption that the global arc volcanism volume was one fourth of the ridge volume [Torgensen, 1989] to obtain a global arc volcanic outgassing flux of 3×10^{12} mol C yr^{-1}. However, this global arc volume is too high by a factor of 2-3 (see compilation by Plank and Langmuir [1998]). We therefore revise Sano and Williams's estimate downward to $F_{arc} = 1.2 \times 10^{12}$ mol yr^{-1}. Marty and Tolstikhin [1998] use similar reasoning to obtain 2.5×10^{12} mol yr^{-1}. We note in passing that the arc volcanic flux is a significant fraction of the crustal metamorphic flux traditionally considered in models of the global CO_2 cycle [Brantley and Koepenick, 1995, Goddéris and François, 1995]. We treat these separately.

Correcting a typographical error (Y. Sano, personal communication, 1996), 75% of the vented C comes from subducted carbonate, 12% comes from organic matter in subducted sediments, and 12% comes from normal mantle. Taken at face value, these imply that some hemipelagic sediments and tectonically eroded crust, which have organic matter as well as pelagic sediments, get subducted and then degassed. In addition, the fraction of CO_2 derived from carbonate shows no obvious correlation with the localities of Plank and Langmuir [1998] where much sedimentary carbonate is subducted. This indicates that significant carbonate is within altered basalt as we discuss below. In a detailed study of Kudryavy volcano on the Kurile islands, Fischer et al. [1998] find that one sixth of the subducted carbonate and one third of the subducted organic carbon are

returned to the surface in arc magmas. We do not consider these fractions to be significantly different. Also, we ignore the true mantle source at arc volcanoes as small compared to uncertainties in F_{ridge}.

Uncertainties in the average arc flux arise because the directly measured flux is dominated by a few volcanoes [Brantley and Koepenick, 1995; Marty and Tolstikhin, 1998]. In particular, the flux from Mount Etna alone is $\sim 1 \times 10^{12}$ mol yr^{-1} of C [Allard et al., 1997]. One might suspect high-level contamination as the crustal region beneath Etna contains sedimentary carbonates and the lavas contain such xenoliths [Michaud, 1995]. This cannot be the whole story because the Etna lavas have mantle helium isotopes and mantle C/He ratios [Allard et al., 1997]. More likely, the present volatile fluxes from Etna are a transient associated with episodic delivery of magma to a high-level chamber. Such transients ought to be included in the long-term global average, but we do not know how frequent or extraordinary they are.

To extrapolate arc fluxes into the past, it is necessary to consider the source of arc volcanism. Arc volcanics are generated when a hydrous fluid is produced by the breakdown of hydrous minerals within the slab. This fluid escapes upward and allows hydrous melting in the mantle wedge within the slab [e.g., Stolper and Newman, 1994]. Incorporation of CO_2 into arc magmas is a complicated result of this process [Huang et al., 1980; Peacock et al., 1994, Peacock, 1996]. Direct breakdown of $CaCO_3$ by reaction with silicates (reaction (1)) to form a CO_2-rich vapor or melt can occur at the relevant depths (~ 100 km) only if the temperature is above $\sim 1300°C$. Thermal calculations, however, indicate that the temperature in subducted material at that depth is typically $< 800°C$ and that temperatures high enough to allow direct melting of ocean crust to form adakite but not direct breakdown of carbonates are rare. CO_2 is somewhat soluble in the hydrous fluid produced within the slab. The fraction of CO_2 entering the fluid is buffered by reactions similar to (1) unless carbonates are so rare that they get used up. In the former case, where carbonate buffers the fluid, the CO_2 outgassing flux is independent of the fraction of carbonate in the subducted basalt but proportional to the amount of fluid released from the basalt. In the latter case, where carbonate is used up, all the CO_2 is outgassed, and so the flux is proportional to the amount of subducted carbonate.

Also affecting extrapolation into the past are higher mantle temperatures [e.g., Nisbet et al., 1993]. The amount of hydrous fluid removed from Archean slabs as voluminous adakite is expected to have been greater than at present [Peacock et al., 1994], and the depth of dehydration to have been shallower. Both of these effects help remove CO_2 from the slab. Pre-plate tectonic crustal overturn is less constrained, but in general, the sinking of any large block would share the same basic thermal features discussed by Peacock et al. papers. In particular, a large overturned surface block is only heated to about the mean of the surface temperature of the Earth and the interior temperature, which is too low for the direct thermal breakdown of carbonates in mafic or ultramafic rock.

To calibrate C_{deep}, we need to consider modern instantaneous fluxes into subduction zones. Going into subduction zones, we have $F_{bas} = 3.4 \times 10^{12}$ mol yr^{-1} and $F_{pel} = 1.4 \times 10^{12}$ mol yr^{-1}; leaving subduction zones, we have $F_{arc} = 1.2 \times 10^{12}$ mol yr^{-1}. As discussed above, we assume $F_{tect} = F_{scrape}$. This leaves $C_{deep} = 75\%$, which agrees with the direct estimate from a Kurile arc volcano of 64-84% [Fischer et al., 1998].

2.3.2. Ridge degassing.

The oceanic crust is a source of CO_2 when magma upwelling at mid-ocean ridges degasses and later is a sink when circulating seawater reacts with the basalt at low temperatures. To describe this process, we discuss the structure of the oceanic crust from the top down. Pillow basalts form when basalt erupts to the seafloor and is immediately cooled by the ocean. At somewhat greater depths, the crust is composed of dikes, which quench quickly to a temperature of a few hundred degrees Celsius and thereafter cool by hydrothermal circulation. At greater depths, magma cools to mostly crystalline mush and then to gabbro. The permeable uppermost crust, the lava flows and the upper dikes, has been traditionally called layer 2A. We follow this convention but note that physical properties change continuously to those of hard rock with depth [e.g., *Hooft et al.*, 1996; *Carlson*, 1998; *Fisher*, 1998]. For bookkeeping purposes we assume that at first, the basalt degasses completely and then, when the basalt is cool, CO_2 is added to it by reaction with seawater. In reality, some igneous CO_2 is retained by the basalt especially within the dike complex. Various authors following *Alt et al.* [1986] report net gain rather than total CO_2 in their flux estimates.

The CO_2 content of the original magma can be inferred from the $CO_2/^3He$ ratio in quenched bubbles, quenched glasses, or hot hydrothermal fluids, and the known total flux of ^3He to the oceans is used to obtain the global CO_2 flux [*Des Marais and Moore*, 1984]. This procedure assumes that helium and carbon dioxide, which have similar solubilities in melt, behave similarly during shallow degassing processes. Various similar estimates have been obtained in this way: 1.0×10^{12} mol yr^{-1} [*Gerlach*, 1991], 2.0×10^{12} mol yr^{-1} [*Marty and Jambon*, 1987], 2.0×10^{12} mol yr^{-1} [*Goddéris and François*, 1995], $2.2\pm0.9\times10^{12}$ mol yr^{-1} [*Marty and Tolstikhin*, 1998], and 2.5×10^{12} mol yr^{-1} [*Zhang and Zindler*, 1993]. The mantle CO_2 abundance is then obtained by assuming that a given thickness of mantle beneath the midoceanic ridge degasses. The *Zhang and Zindler* [1993] flux and mantle reservoir, 18×10^{21} mol, for example, are equivalent to a degassing depth of 56 km, the preferred degassing depth of *Langmuir et al.* [1992] and a depth which is constrained independently of volatiles. Currently, the timescale to cycle the mantle through the 56 km deep melting zone at the current rate of seafloor spreading is 7.2 billion years, longer than the age of the Earth. Such slow recycling of the mantle is compatible with its degassing history obtained from the systematics of radiogenic ^{40}Ar, which had not yet formed early in the Earth's history [*Sleep*, 1979; *Williams and Pan*, 1992; *Tajika and Matsui*, 1993; *Phipps Morgan*, 1998]. In particular, much of the mantle has escaped degassing during the last 3.5 b.y. because it has not passed through a magma source region of a mid-oceanic ridge and not because it is somehow nondegassable. Therefore we do not include a nondegassable part of the mantle in our models as did *Zhang and Zindler* [1993]. It plays little part in their CO_2 cycle and would add an ill-constrained parameter to our models.

The degassing flux is proportional to the volume of material cycled through time through the mantle source region of magmas and to the CO_2 concentration in this region. That is, the source is proportional to the global rate of crustal production $\partial A/\partial t$ and to the amount of CO_2 in a unit column of mantle material degassed to a source depth D_s.

$$F_{ridge} = \frac{\partial A}{\partial t}\frac{D_s\rho_s}{\rho_m}\left(\frac{R_{man}}{V_{man}}\right) = \frac{\partial A}{\partial t}\left(\frac{R_{man}}{V_{ridge}}\right)D_s ,\qquad (10)$$

where ρ_s is the density of the degassed mantle, ρ_m is the

average mantle density, and V_{man} is the volume of the mantle. The current degassing depth D_s is well constrained at ~56 km . The effective ridge volume constant V_{ridge} is 1.2×10^{12} km^3. It changes little once the Earth and its core have formed. Reliable estimates of the present flux F_{ridge} range between 1.0 and 2.5×10^{12} mol yr^{-1}. These yield a present mantle reservoir between 7and 18×10^{21} mol. Reliable estimates for the flux from plume-derived hotspot magmas are not available. *Marty and Tolstikhin* [1998] give an upper limit of 3×10^{12} mol yr^{-1} and a negligible lower limit. We do not consider hotspots separately.

2.3.3. Hydrothermal carbonatization 1

The oceanic crust is a sink for CO_2 by (1). At low temperatures, circulating seawater reacts with basalt in layer 2A to form carbonates. Direct evidence for this process exists. Carbonate veins and disseminated carbonate formed in this way have been sampled from the small number of holes that have been drilled deeply into the oceanic crust [*Alt and Teagle*, 1999]. The irregular distribution of carbonate within holes and variations between closely spaced holes hinders direct extrapolation to the global cycle. An integrated approach using geochemistry and heat flow along with the samples is perhaps more practical.

The amount of carbonate added to the oceanic crust can be constrained by chemical analyses of hydrothermal fluids and by using the fluxes of heat and various elements to calibrate the total volume of flow [e.g., *François and Walker*, 1992; *Alt*, 1995, *Caldeira*, 1995; *Kadko et al.*, 1995, *Stein et al.*, 1995; *Brady and Gislason*, 1997; *Sansone et al.*, 1998]. For this purpose, we follow *Schultz and Elderfield* [1997, 1999] and partition hydrothermal circulation into three regimes: high temperature, ~350°C, axial flow; warm, ~20°C, near-axial flow which extensively reacts with the rock; and cool, ~5°C, off-axial flow through the shallowest ocean crust. The high-temperature flow serves to carry CO_2 from the hot basalt into the ocean. The cold flow circulates through a relatively small volume of very shallow crust and is not believed to be significant to the CO_2 cycle.

The warm flow appears to be an important CO_2 sink. The chemistry of the warm and less reacted cool waters has proved more difficult to study than the hot waters leaving black smoker vents. Both warm and cold waters have been sampled in the subsurface [*Mottl and Wheat*, 1994]. Dissolved CO_2 has been measured from a warm vent on the flank of the Juan de Fuca ridge and found to be 66% depleted relative to normal seawater [*Sansone et al.*, 1998].

The flux of warm seawater W (in units of volume per time) through the oceanic crust can be estimated from the measured global seafloor heat flow anomaly H (in units of heat per time) and the temperature anomaly T_w of the hydrothermal seawater relative to the bottom of the ocean. The heat flow anomaly refers to the difference between the heat flow expected from the cooling oceanic crust (which declines with the square root of age) and the heat flow obtained by directly measuring the temperature gradient and conductivity in the sediments. The difference is ascribed to hydrothermal cooling: H amounts to ~20% of the global oceanic heat flow and occurs mostly in young (<1 m.y.) crust, for which the thermal gradient is steep enough that circulating water can reach warm rock. For the flow of water we write

$$W = \frac{H}{T_wC_w\rho_w} ,\qquad (11)$$

where ρ_wC_w = 4 MJ m^{-3} is the heat capacity per unit volume of water. H can be expressed in terms of the rate that warm new crust is created and the degree to which hydrothermal circulation

cools it. New crust is created at the rate $\partial A/\partial t$, currently 3 km^2 yr^{-1}. The flux of CO_2 into the warm crust is therefore

$$F_{\text{hydro}} = R_{\text{oc}}\left(\frac{W}{V_{\text{oc}}}\right) = \frac{H}{\rho_w C_w T_w}\left(\frac{R_{\text{oc}}}{V_{\text{oc}}}\right) \equiv \frac{\partial A}{\partial t}\frac{R_{\text{oc}}}{A_{\text{hydro}}} \quad , \qquad (12)$$

in which V_{oc} refers to the volume of the oceans and $A_{\text{hydro}} = (\partial A/\partial t)(V_{\text{oc}}/W)$ is a constant with units of area.

In practice, W is directly inferred from heat flow and chemical mass balances. Warm hydrothermal flow is a major sink for dissolved oceanic Mg^{+2}. The Mg^{+2} in the warm hydrothermal fluid is removed quantitatively by reaction with basalt. Because the flux of Mg^{+2} into the ocean in river waters and the competing sinks (e.g., clays) can be estimated, mass balance and the known Mg^{+2} concentration in seawater can be used to determine the required warm hydrothermal flux W. This argument is independent of CO_2.

Using both heat flow and magnesium, *Schultz and Elderfield* [1997, 1999] conclude that 1.5×10^{12} W, or about a quarter of the total global hydrothermal heat flow, escapes through warm vents with an assumed average temperature anomaly of 20 K; the corresponding flux of water is $W=6.4\times10^{11}$ m^3 yr^{-1}. The latter implies that the entire ocean circulates through warm vents in 2 million years, for which $A_{\text{hydro}}=6\times10^6$ km^2. In the current ocean a hydrothermal flux equivalent to quantitative extraction of CO_2 on a cycle time of 2 m.y. is $F_{\text{hydro}}=1.65\times10^{12}$ mol yr^{-1}. On the other hand, using similar data, *Sansone et al.* [1998] argue for warmer vents—temperature anomaly 64 K, that carry a somewhat smaller fraction, 8-20%, of the global hydrothermal heat flow. Their estimates translate into lower water flows and longer cycle times, between 8 and 20 m.y., for which $2.4\times10^7<A_{\text{hydro}}<6\times10^7$ km^2. *Walker* [1985] uses 10 m.y. for this cycle. As the actual flux is uncertain, we shall use *Schultz and Elderfield's* [1997, 1999]

estimate as an upper limit. We also present results based on the lowest of *Sansone et al.'s* [1998] estimates as our lower limit.

2.3.4. Balanced mantle cycles. The simplest case is to consider the steady state value of R_{oc} that results from equating mantle outgassing to ingassing by subduction. From (7), the condition for steady state is $F_{\text{ridge}}=C_{\text{deep}}(F_{\text{hydro}}+F_{\text{ej}})$. Using (10) for F_{ridge} and (12) for F_{hydro} we obtain a steady state reservoir size of

$$\langle R_{\text{oc}}\rangle = \frac{A_{\text{hydro}}}{\partial A/\partial t}\frac{\partial A}{\partial t}\frac{R_{\text{man}}D_s}{V_{\text{ridge}}C_{\text{deep}}} = \frac{A_{\text{hydro}}D_s}{V_{\text{ridge}}C_{\text{deep}}}R_{\text{man}} \quad , \qquad (13)$$

which is independent of the rate of crustal overturn. The current steady state value is 2.9-7.4×10^{18} mol assuming that $D_s=56$ km, R_{man} is in the range given above, $V_{\text{ridge}}=1.2\times10^{12}$ km^2, $A_{\text{hydro}}=6\times10^6$ km^2, and $C_{\text{deep}}=0.75$. This is near the current amount of 3.3×10^{18} mol. What is interesting about this result is (1) that it is obtained on the basis of geological and geochemical arguments in which CO_2 plays no part and (2) that it completely ignores the continents and the Urey cycle. Fluxes associated with this balanced cycle are shown in Figure 4. Increasing A_{hydro} by a factor of 4-10, in line with the *Sansone et al* [1998] results, increases the steady state value of R_{oc} by a factor of 4-10. The latter is within the range obtained for the past 400 m.y. by *Ekart et al.* [1999].

2.3.5. Hydrothermal carbonatization 2. To extrapolate F_{hydro} into the past requires a model of the water-rock reaction. There are two important possibilities, depending on whether the reactable cations are more or less abundant than CO_2. In (13) we have implicitly assumed that CO_2 is quantitatively removed from low-temperature hydrothermal fluids. In effect we presume fast reactions with a superabundance of cations. *Walker* [1985] and *François and Walker* [1992] assume that CO_2 is removed in
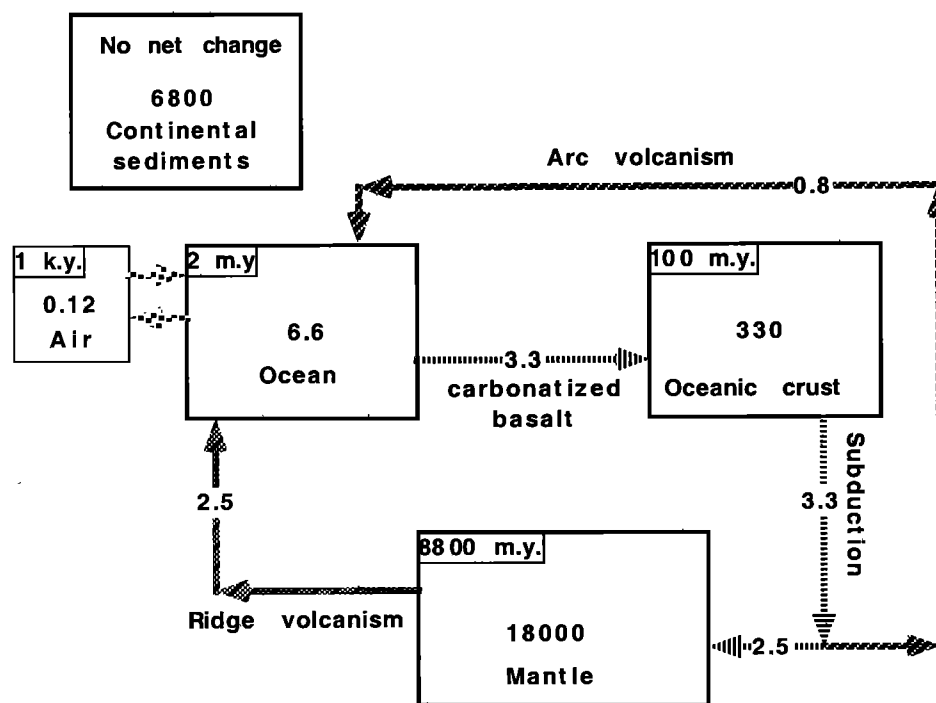
Figure 4. A balanced version of the modern CO_2 cycle, shown with reservoirs (boxes) and fluxes (arrows). Current residence times are shown in the corners of the reservoirs which actively partake. The continental reservoir experiences no net change, although it exchanges with the other reservoirs.

linear proportion to its concentration. In effect, they presume that CO_2 reacts slowly and incompletely with abundant cations. This is equivalent to assuming that a constant fraction of the water flux W becomes quantitatively depleted in CO_2, and thus their model differs from ours only in the value of A_{hydro}. In either case it is the rate that CO_2-rich waters are delivered to the oceanic crust by hydrothermal circulation that limits uptake, so that we may take CO_2 as being quantitatively depleted in the circulating seawater until available CaO, MgO, and FeO in the rock are exhausted.

However, there is some experimental evidence that water-rock reaction kinetics are not strongly dependent on CO_2 or on reasonable variations in pH [*Caldeira*, 1995; *Brady and Gislason*, 1997]. In these cases reaction rates are limited by the availability of cations. If so, then it is possible that the uptake of CO_2 by the ocean floor has always been similar to what it is at present, as is assumed in the models of *Caldeira* [1995], *Goddéris and François* [1995], and *Brady and Gislason* [1997]. This would make the current rough equality between subduction and ridge degassing (13) a coincidence and leave as an open puzzle how the mantle CO_2 cycle is to be closed over long timescales.

In view of these uncertainties, we will write F_{hydro} where the parameter α represents the dependence of hydrothermal carbonatization on pCO_2. Quantitative depletion corresponds to $\alpha = 1$. *Brady and Gislason*'s [1997] laboratory data correspond to $\alpha = 0.23$.

We can test these assumptions at a higher CO_2 concentration by comparing reconstructed CO_2 levels to the observed carbonate in Mesozoic ocean cores. As noted, quantitative extraction of CO_2 in the current over 2 m.y. corresponds to $F_{hydro} = 1.65 \times 10^{12}$ mol yr^{-1}. This upper limit on F_{hydro} is compatible with what is known about the abundance of carbonate from holes drilled into layer 2A of the oceanic crust. By all accounts, CO_2 levels were higher in the Mesozoic than at present [*Lasaga et al.*, 1985; *Berner* 1994, 1997; *Ekart et al.*, 1999]. Available data hint that the carbonate content of Mesozoic seafloor was also higher than at present, but interpretation is complicated by sampling bias. First, the older high-carbonate samples have obviously had longer to alter and might be high for that reason [*Alt and Teagle*, 1999]. However, most of the alteration and the warm hydrothermal circulation occur near the ridge axis when the crust is young [see *Carlson*, 1998]. Second, as noted by *Alt* [1993], the easily weathered layer of pillow basalts and fractured dikes is thicker at slow spreading ridges than at fast ones. As expected, there is more carbonate in samples from slow ridges than in samples from fast ridges [*Alt*, 1993, Figure 8]. This tendency may be somewhat offset by a countering tendency for the deep part of the dike complex at fast ridges to trap magmatic CO_2. Such trapping is indicated by data from 800 to 1800 m deep in the crust at Hole 504B; see *Alt et al.* [1996b, Figures 5 and 6]. Finally, there is a relative factor of a few variation in carbonate abundance between nearby Holes 504B and 896A [*Alt et al.*, 1996a], which indicates that it is difficult to obtain a reliable average. *Sansone et al.* [1998] give further discussion of this unresolved topic. We think it more likely that young samples have less carbonate because there was less CO_2 in seawater when they formed rather than because they have not yet had time to react. That is, our estimated subduction flux is the weighted average of crust now being subducted, not crust now being formed.

We will use $F_{bas} = 3.4 \times 10^{12}$ mol yr^{-1} as the flux of carbonate in carbonatized oceanic crust currently entering subduction zones. This is *Alt and Teagle*'s [1999] estimate of the average for currently existing oceanic crust obtained by a more thorough review of data on carbonate samples from bore holes into the oceanic crust. It approaches *Zhang and Zindler*'s [1993] estimate of 4×10^{12} mol yr^{-1}, which is based on measurements of CO_2 [*Staudigel et al.*, 1989, 1996] in older crust formed at fast ridges in the Pacific that is about to be subducted. These high estimates are consistent with the observation, noted above, that a significant carbonate source is needed at modern subduction zones where pelagic carbonate is not being subducted.

That F_{bas} exceeds the upper limit on the current value of F_{hydro} implies that flow rates are probably fast and CO_2 reaction rates nearly quantitative at present. Using $\alpha = 1$, $F_{bas} = 3.4 \times 10^{12}$ mol yr^{-1} implies that the Mesozoic oceans contained $\sim 7 \times 10^{18}$ mol of CO_2. This is comparable to *Lasaga et al.*'s [1985] estimate of 10×10^{18} mol of CO_2. (Lasaga et al.'s models go back to 100 Ma and not all the way to the age 118 Ma [*Donnelly et al.*, 1979] of the *Staudigel et al.* [1989, 1996] samples.) On the other hand, *Ekart et al.*'s [1999] more direct estimate from paleosol data that pCO_2 was as high as 8 PAL in the Mesozoic is consistent with $\alpha < 1$ for CO_2 levels higher than the present.

Speeding up the global rate of crustal production proportionally increases the ridge alteration flux. As parameterized here, hydrothermal alteration buffers the build up of dissolved CO_2 in the ocean. This buffering property has not been included in several models of the CO_2 cycle. *Caldeira* [1995], *Goddéris and François* [1995], and *Brady and Gislason* [1997] all assume that the carbonate flux depends on the kinetics of rock-water reactions and that these kinetics depend quite weakly on the CO_2 content of the water. The possibility of using other Cenozoic cycles to indirectly constrain basalt-CO_2 kinetics is noted by *Goddéris and François* [1995] and *François and Goddéris* [1998]. This requires assumptions about the rate-limiting steps for the rock-water reactions.

2.3.6. Oceanic pH. Oceanic pH controls the partitioning of CO_2 between the ocean and the atmosphere and hence the pCO_2 obtained from a given reservoir size R_{oc}. That is, decreasing pH by one unit increases pCO_2 by a factor of 10 when most of the CO_2 in R_{oc} is in the ocean. Oceanic pH also enters implicitly in our cycle calculations, which assume that the bulk of the ocean plus atmosphere reservoir is in the ocean. This is true as long as the pH is not more acid than ~ 6.5 [*Walker*, 1985]. A short discussion of the factors affecting oceanic pH is in order.

Over geological times, the pH of the modern ocean is dynamically buffered by low-temperature weathering and seafloor alteration of silicates (which produces alkaline waters) and high-temperature axial hydrothermal circulation (which produces acid waters) [e.g., *Grotzinger and Kasting*, 1993]. High-temperature acid waters escape from black and white smoker vents. The pH can get as low as 3 [*Schultz and Elderfield*, 1997, 1999]. This balance gives a useful analog to the early ocean. Low-temperature alteration of mafic and ultramafic rocks produce alkaline waters in both fresh and saline conditions [*Kempe and Degens*, 1985; *Kempe and Kazmierczak*, 1994]. This is most easily observed on land. The processes that form alkaline brines are sinks for atmospheric CO_2. Vein carbonates in the rocks attest to this.

The relative importance of high-temperature and low-temperature vents on the early Earth and hence the pH of the early ocean is not agreed upon. *Kempe and Kazmierczak* [1994] note that impact ejecta and vigorous tectonic activity on the early Earth would have exposed much more rock to low-temperature alteration and that fluids reacting with Archean komatiitic lavas are more alkaline than those reacting with modern basalts. They contend that the early ocean was significantly more alkaline than present. *Macloed et al.* [1994] and *Russell and Hall* [1997], in

contrast, focus on the large amount of hot hydrothermal activity on the early Earth and contend that the early ocean was acid and that low-temperature hydrothermal vents served only to produce local alkaline conditions.

Direct evidence to support either position is, at best, model dependent. We have no strong reason to expect the relative proportions of high- and low-temperature hydrothermal systems to differ between the Archean (or even the Hadean) and today. In particular, the bulk of both the low- and high-temperature alterations occur within young crust near the ridge axis, implying that the life time of oceanic crust is not a major factor. It is a reasonable compromise for the present to regard pH as fixed in our calculations. This has little effect on the computed cycles as long as the pH is high enough that there is much more CO_2 in the ocean than in the air.

3. Ancient CO_2 Cycle

Extrapolating the CO_2 cycle into ancient times requires us to first consider what happens when plate tectonic cycles run more quickly and then, for earlier times, to consider effects that are no longer important on Earth. In order of increasing ancestry and uncertainty, we consider higher heat flows and related issues within the constraints of plate tectonics and then abundant impact ejecta as a major source of easily weathered and subductable mafic materials. Other topics related to the earliest Earth, including transient runaway greenhouse atmospheres and CO_2 cycling before some form of subduction existed, are beyond the scope of this paper. We begin with a time in the Archean when the effects of impacts were no longer significant.

3.1. Archean Cycle

The steady state value of R_{oc} in (13) provides a preliminary estimate of CO_2 in the Archean ocean. The constants V_{ridge} and A_{hydro} vary little. The degassing depth D_s, as noted above, is expected to be much greater in the past when the upwelling mantle was hotter. For purposes of illustration, we double D_s to 112 km using the melting temperature from *Langmuir et al.* [1992] and the inference that the mantle was 150 K hotter in the middle and late Archean [*Abbott et al.*, 1994]. We arbitrarily divide C_{deep} in half to 3/8 to represent more efficient degassing of crust overturned into hot mantle. The Archean crustal CO_2 reservoir is unknown but not critical to the discussion as it enters (13) only through the mantle mass. For example, if, for simplicity, we assume there were no large crustal reservoirs, the steady state value of oceanic carbonate $<R_{oc}>$ increased only by a factor of the total size, 14-25×10^{21} mol, divided by the current mantle size of 7-18×10^{21} mol, i.e., ~ 1.4-2.0. Altogether, these modifications have the effect of increasing $<R_{oc}>$ in (13) by a factor of 5.6-7.9, to 23-41×10^{18} mol for fast hydrothermal cycling (current $\tau_{hydro}=2$ Ma) or to 230-410×10^{18} mol if hydrothermal cycling is slow (20 Ma). Thus even inefficient hydrothermal sinks buffer oceanic CO_2 to levels less than ~ 100 PAL.

In order to go beyond the illustrative example, we solve the time-dependent problem with the coupled (4), (5), and (6) using the value of R_{oc} obtained assuming steady state in (3). The simplifying assumptions of ignoring the carbonate weathering and precipitation cycle in (3) and (5), ignoring pelagic deposition in (3) and (4), and ignoring tectonic erosion and offscraping in (4) and (5) are again made. To include the Urey cycle, values of R_{oc}, T, and pCO_2 are obtained from (8a) and (3); F_{meta} is proportional to $Q^a R_{con}$ where a is 1. As in (13), we use (10) for

F_{ridge} and (12) for F_{hydro}. We take $\partial A / \partial t \propto Q^\alpha$, $D_s = 56$ km ($1+t/3$ Ga) for $t < 3$ Ga and $D_s = 112$ km for $t > 3$ Ga, and C_{deep} inversely proportional to D_s. We will take $F_{hydro} \propto R_{oc}{}^\alpha$ where α (analogous to β in (8a) and (8b)) is the exponent representing the dependence of basalt reaction rates on pCO_2. The latter parameter allows us to address models in which hydrothermal reactions are not strongly dependent on pCO_2.

We calibrate the models to give the current crustal reservoir R_{con} and an average pCO_2 over the past 400 m.y. of 3 PAL. We can do this by adjusting any two of four parameters. These four are the current hydrothermal circulation A_{hydro} the dependence of seafloor uptake on pCO_2, represented by α the calibration of silicate weathering C_{SiO2w} and the size of the mantle reservoir R_{man}. The latter is directly proportional to the mid-ocean ridge outgassing flux F_{ridge}. The mantle degassing time and the degassing depth D_s are not free parameters because they are constrained independently of CO_2. Of these four, A_{hydro} and F_{ridge} are observables subject to constraints discussed above in sections 2.3.3 and 2.3.2. The power α may be near unity, but for our purposes it is best regarded it as free, as together with A_{hydro} it determines the return flux to the mantle.

Figure 5 shows loci of successful models as functions of the obserables A_{hydro} (the inverse of τ_{hydro}) and F_{ridge} (equivalent to R_{man}). Lines are labeled by the ill-constrained α. The fourth parameter C_{SiO2w} tunes the Urey cycle and needs to be set separately for every model. In successful models, F_{SiO2w} is typically $\sim 10\%$ smaller than F_{meta}. Initial conditions are wholly unimportant, but plant roots can be important, if roots actually have a large effect on weathering. This latter issue will be returned to in section 3.1.5. The standard models (solid lines) are labeled "faint Sun" to indicate that they obey the predictions of standard stellar evolution theory. The models labeled "bright Sun" will be discussed below in section 3.1.3.

Indicated on Figure 5 are two models with $F_{ridge}=2 \times 10^{18}$ mol yr^{-1} and different values of τ_{hydro} and α. These models have correspondingly smaller current mantle inventories of CO_2 ($R_{man} = 1440 \times 10^{18}$ mol) than those used in Figures 2 and 4. We will discuss these two models in detail. The models are chosen to compare strong ($\alpha = 1$) and weak ($\alpha = 0.4$) dependence on pCO_2. For the first of these models ($\alpha = 1$) we require that currently, $A_{hydro} = 2.6 \times 10^7$ km^2 (equivalent to recycling R_{oc} every 8.7 m.y.) and silicate weathering comparable to that of the mantleless models in Figure 3. The second model ($\alpha = 0.4$) uses faster hydrothermal cycling, $A_{hydro} = 6.3 \times 10^7$ km^2 (2.1 m.y.), and silicate weathering $\sim 10\%$ slower than for Figure 3.

Computed reservoir sizes for these two cases (labeled by $\alpha = 1$ and $\alpha = 0.4$) are the subjects of Figures 6a and 6b. After an initial (and quickly forgotten) transient caused by the arbitrary starting values (we set the initial values to their present values), the reservoir sizes evolve gradually and independently of the starting conditions. Ejecta are included in the models and are discussed in the context of the Hadean (section 3.2). The Archean and later behavior is weakly dependent on the starting conditions and the amount of ejecta. In both models, the crustal carbonate reservoir builds up over time. Accompanying fluxes are shown in Figures 7a and 7b. The Urey fluxes from silicate weathering and metamorphism increase with time for $\alpha = 1$ but are nearly constant for $\alpha = 0.4$. This indicates that the Urey cycle has greater influence later in the Earth's history, as might be expected. Note that the silicate weathering flux is small compared to the hydrothermal flux at times where the computed temperatures are below freezing. The failure of our parameterization to precisely represent glacial conditions thus
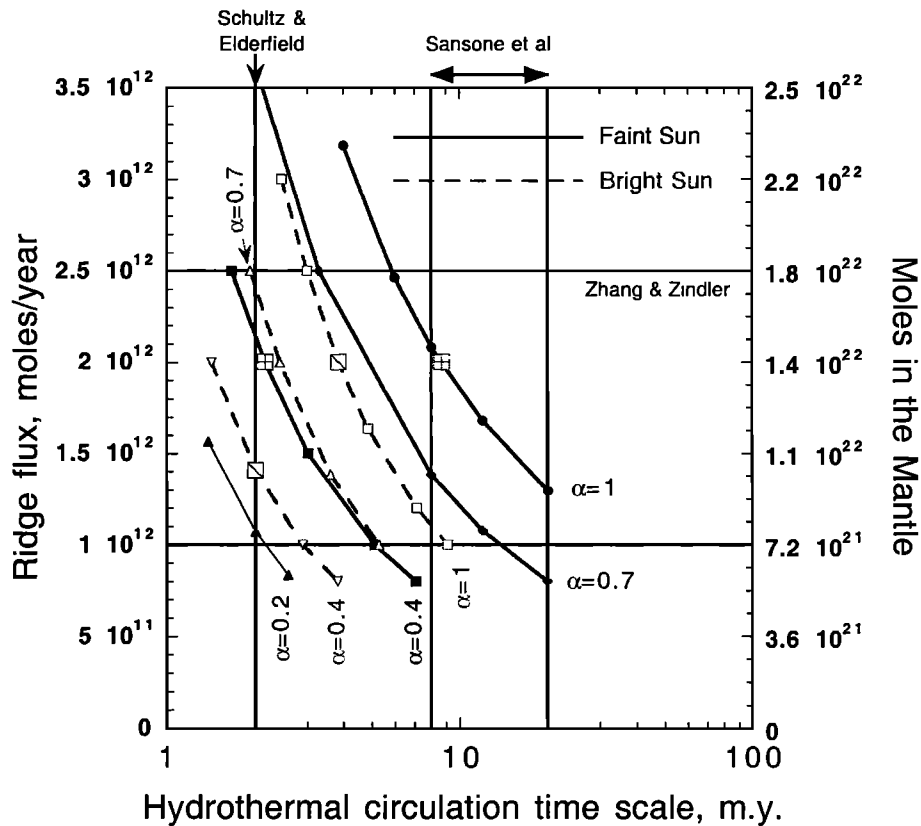
Figure 5. Loci of current parameter choices that can recreate the modern atmospheric and continental CO_2 inventories for our standard "faint Sun" model and for warmer "bright Sun" models. Estimated timescales for circulating the ocean through warm oceanic basalt range between 2 and 20 m.y. The ridge flux represents mantle degassing of CO_2. Estimates put this in the range $1\times10^{12} < F_{ridge} < 2.5\times10^{12}$ mol yr^{-1}. This range is equivalent to mantle inventories $7\times10^{21} < R_{man} < 18\times10^{21}$ mol. The parameter α represents the dependence of seafloor carbonitization on the concentration of CO_2 in seawater. Faint sun describes the canonical course of solar evolution (λ=1, (14)). For bright Sun we have arbitrarily reduced the rate of solar luminosity evolution by a factor of 5 ($\lambda = 0.2$, (14)). These serve either to illustrate the effects of a less faint ancient Sun, or, perhaps more palatably, as a proxy for the influence of an additional potent greenhouse gas or gases. The models indicated by large squares are presented in more detail in Figures 6, 7, 8, and 10.. Note that bright Sun models require less carbon in the mantle.

does not matter much in obtaining pCO_2. The computed temperatures, however, do depend on the greenhouse parameterization, which does not explicitly include glaciation.

Computed histories of pCO_2 and surface temperature are shown in Figures 8a and 8b, respectively. In both models, pCO_2 decreases with time, and temperature increases after the Hadean. Archean surface temperatures are temperate for $\alpha = 0.4$ and cold for $\alpha = 1$.

3.1.1. Availability of alterable oceanic crust. The CO_2 cycle may have been also affected by the finite volume of reactable oceanic crust. Crudely basalt is 10% by mass of each of MgO, CaO, and FeO. A half kilometer of basalt, a thickness comparable to the modern permeable and reactable layer 2A at fast ridges (it is somewhat thicker at slow ridges e.g., [*Hooft et al.*, 1996]), if fully carbonatized would yield 300 m of carbonate, or 3×10^{21} mol. The latter is about half of the present total crustal inventory. This limit is not exceeded in the models in Figures 8a and 8b. It would be exceeded early in the model if C_{deep} were then less than ~0.2, which is about half the value we use in our models. If C_{deep} were too small, CO_2 could not be subducted at the rate it was degassed. Rather, it would build up in crustal

carbonate reservoirs and, if these reservoirs were filled to capacity, in the atmosphere and ocean. For comparison, our lower and upper limits on the current inventory of carbonatized basalt are equivalent to 4 and 40 m of carbonate, respectively (i.e. ~1-10% carbonatization). Thus the finite capacity of the oceanic crust to take up carbonate imposes a serious upper limit on F_{hydro}.

The limited cation content of layer 2A has implications for α. That most of the CO_2 is removed from warm vent fluids [*Sansone et al.*, 1998] is the strongest argument that α for hydrothermal circulation is currently near unity. This can be reconciled with carbonatization levels of <10% but is obviously unsustainable if carbonatization levels get much higher. We would expect the depth of the carbonatized layer to grow as CO_2 levels increase, but this growth occurs by reaction of increasingly impermeable media, which implies that $\alpha < 1$ if there is a lot of CO_2.

The chemistry of the circulating water changes as CaO, MgO, and FeO in the rock are used up in that order. There is much evidence that massive carbonatization occurred on the early Earth. Carbonatized igneous rocks are found in the oldest Archean terrains [*deWit and Hart*, 1993; *Nutman et al.*, 1996], and carbonatized volcanic rocks are common in general in the
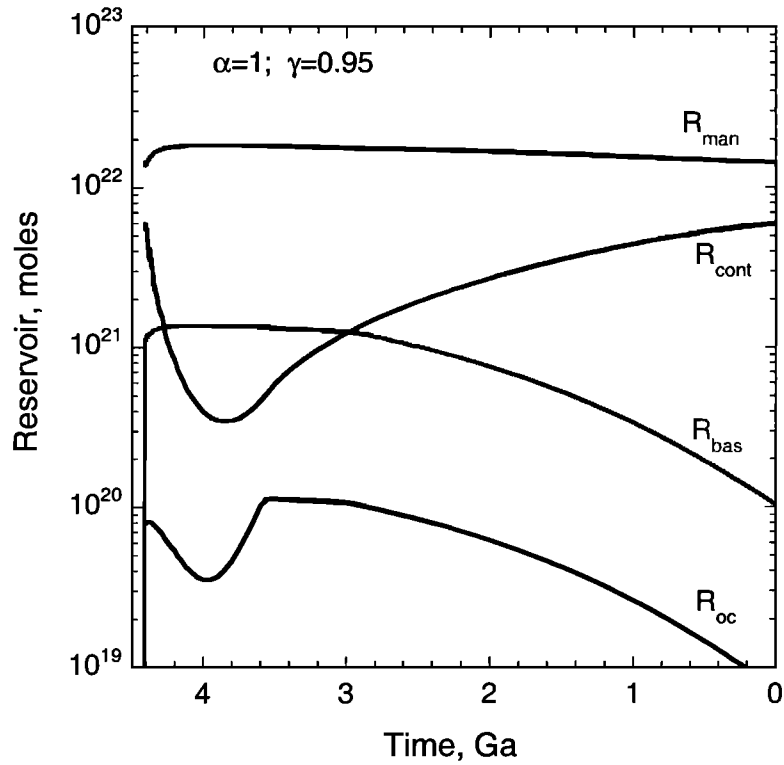
Figure 6a. Reservoir sizes, shown as functions of time for the faint Sun model with $\alpha=1$. Model parameters are indicated on Figure 5. The model starts with the current values for the continental and mantle reservoirs. This assumption is arbitrary but unimportant: after an initial transient. The basalt reservoir in the Hadean includes ejecta on the seafloor modeled with $\gamma = 0.95$.
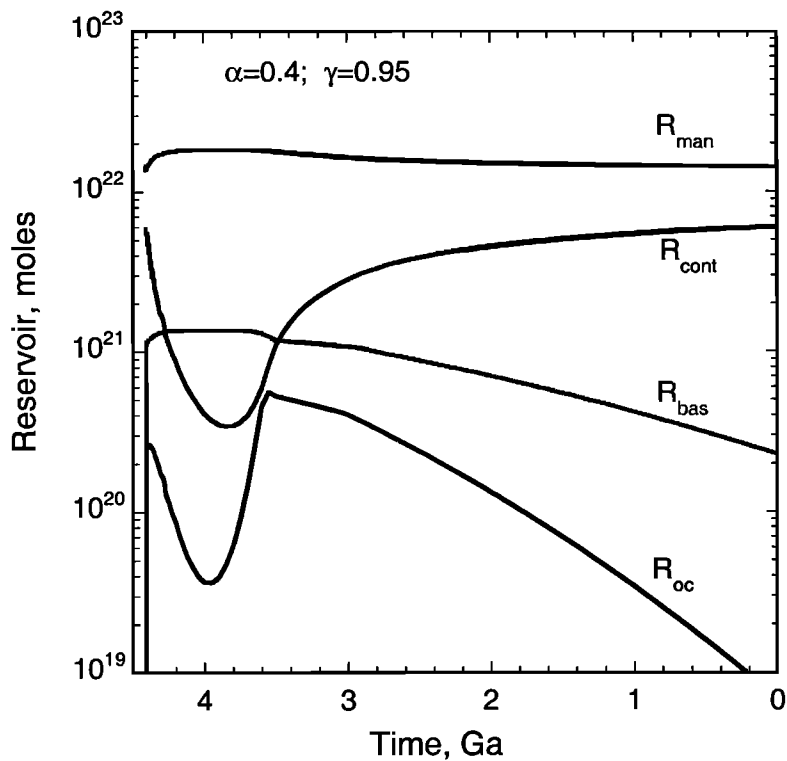

Figure 6b. Reservoir sizes, shown as functions of time for the faint Sun model with $\alpha=0.4$. The continental crustal reservoir grows more rapidly with $\alpha=0.4$ than with $\alpha=1$.
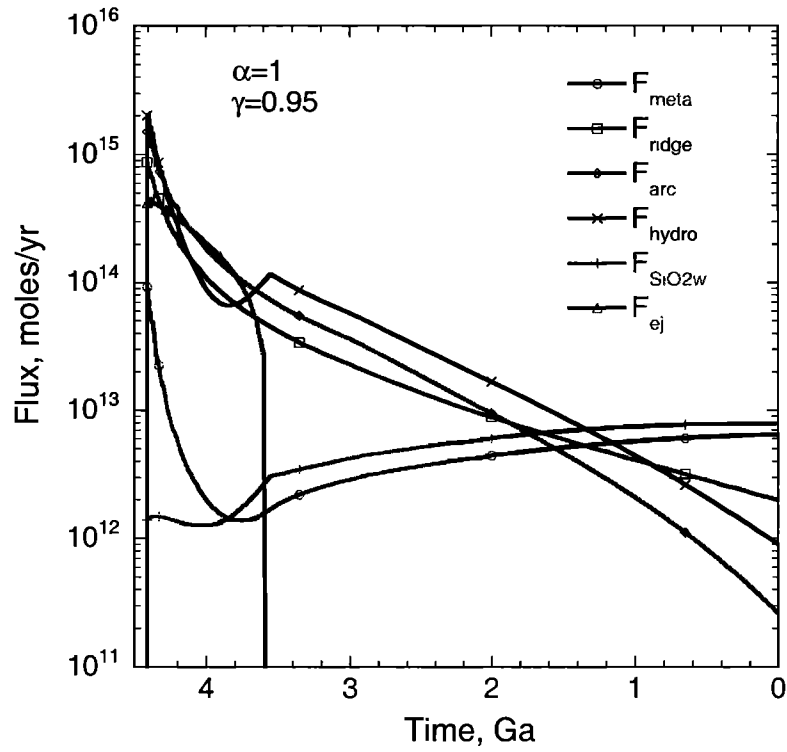
Figure 7a. Fluxes between reservoirs for the faint Sun model with $\alpha=1$. Crustal fluxes from silicate weathering and metamorphism increase with time, while mantle fluxes decrease.
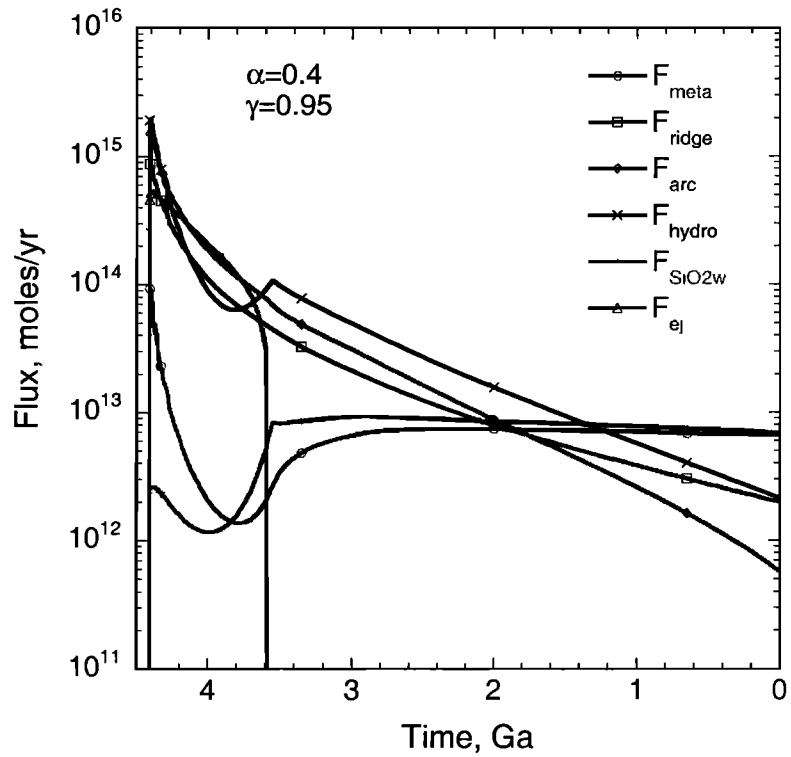
Figure 7b. Fluxes between reservoirs for the faint Sun model with $\alpha=0.4$. Crustal fluxes from silicate weathering and metamorphism change slowly after 3 Ga.
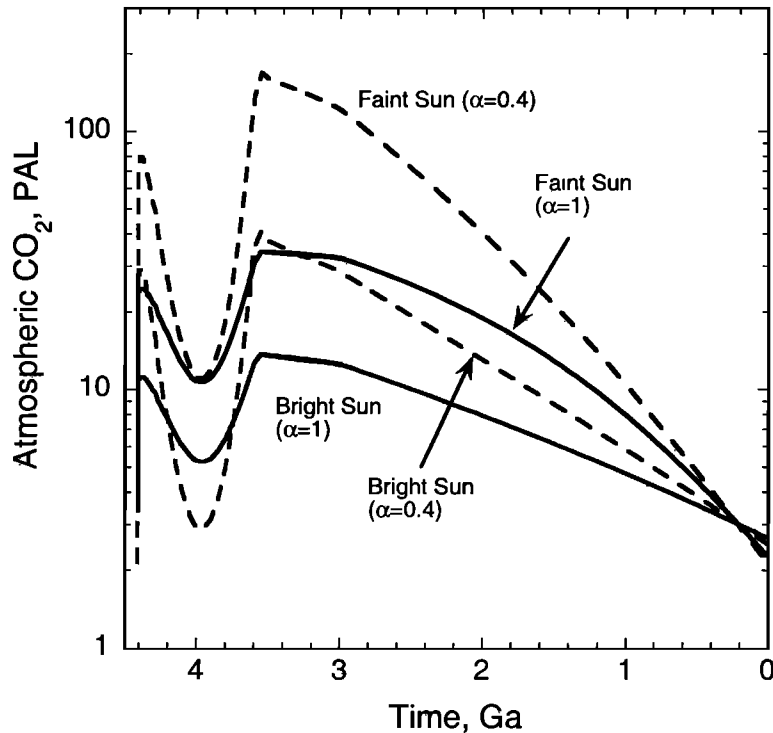
Figure 8a. Atmospheric CO_2 (pCO_2) histories for both seafloor weathering rates ($\alpha=1$, dashed lines; $\alpha=0.4$, solid lines) and for both solar evolution histories. All the models include impact ejecta in the Hadean, modeled here with $\gamma = 0.95$. The bright Sun produces warmer climates (Figure 8b) that speed silicate weathering, significantly reducing pCO_2 and thereby indicating that silicate weathering has a significant effect throughout Earth's history.
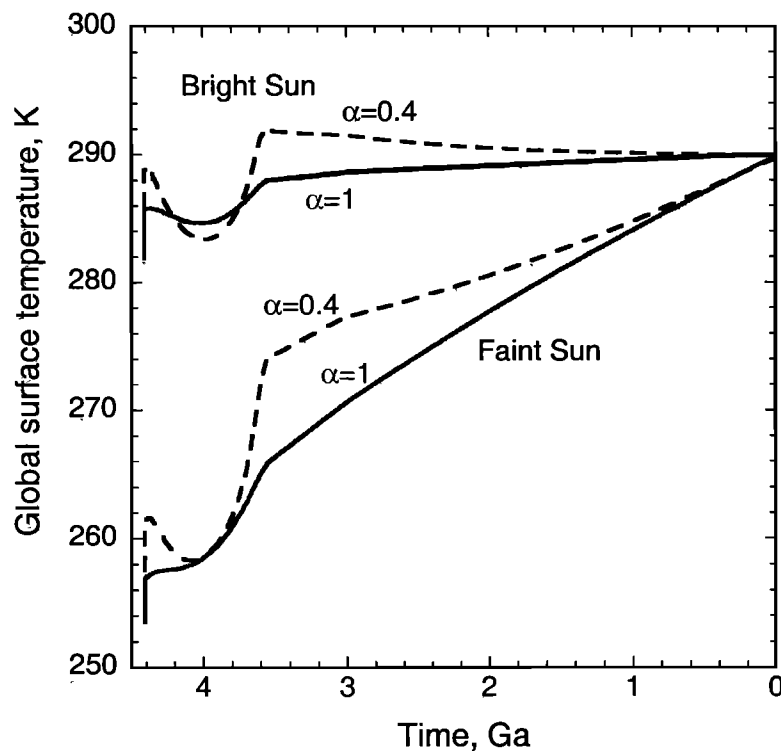
Figure 8b. Global surface temperature histories for both seafloor weathering rates ($\alpha=1$, dashed lines; $\alpha=0.4$, solid lines) and for both solar evolution histories. All the models include impact ejecta in the Hadean, modeled here with $\gamma = 0.95$.

Archean [*Lowe*, 1997]. Silicified volcanic rocks are also common in the Archean [*Nutman et al.*, 1996; *Lowe*, 1997]. The cations leached from these rocks would have formed carbonates elsewhere, either in veins or sediments. The reality of $FeCO_3$ formation is indicated by the occurrence of siderite pseudomorphs after olivine in Archean komatiites (E. Nisbet, personal communication, 1999).

3.1.2. Growth of continental reservoir.
The models presented in Figures 6a and 6b have the continental reservoir growing except for early in the Earth's history. This occurs even though we keep the nominal area of continents constant. This feature occurs because the mantle cycle lowers pCO_2 below the level that would be maintained by the Urey cycle acting alone. This reduces the silicate weathering flux. CO_2 once liberated from the continent by metamorphism then tends to end up in the oceanic crust and get subducted.

A more sophisticated way of representing continents might seem in order. Growth of the continental reservoir requires significant places to deposit and store carbonates on continental platforms. Storage sites that are rarely affected by metamorphism would work best. In this way the continental reservoir might be viewed as a bucket with a finite capacity. At times when space for carbonates is available on platforms, carbonate deposits will, over a modest time, fill the available space. Once these safe places are filled, subsequent deposits would form in regions prone to metamorphism. The capacity of the bucket would be coupled to sea level variations. We recognize that such behavior may be important on moderate timescales where the mantle cycle does not greatly change the crustal reservoir.

3.1.3. Effect of other greenhouse gases.
Both the $\alpha = 0.4$ and the $\alpha = 1$ models violate the constraint on pCO_2 from the lack of siderite in paleosols dated 2.2-2.75 Ga [*Rye et al.*, 1995] (Figure 9). The reason for this is that the *Caldeira and Kasting* [1992] climate parameterization for 2.75 Ga lies above the siderite stability curve except for temperatures well below freezing. There are three possible solutions for this. (1) The paleosol may represent a local region where the temperature was higher than the global average, or it might just represent a few warm seasons when the temperature was higher than the global average plotted on Figure 9. The timing bias is significant at present [*Ekart et al.*, 1999]. Reactions occur mostly during the warm months of the year, when siderite is less stable. They find that paleosol formation temperature may be as much as 20 K above the mean annual temperature at high latitudes and 10 K in
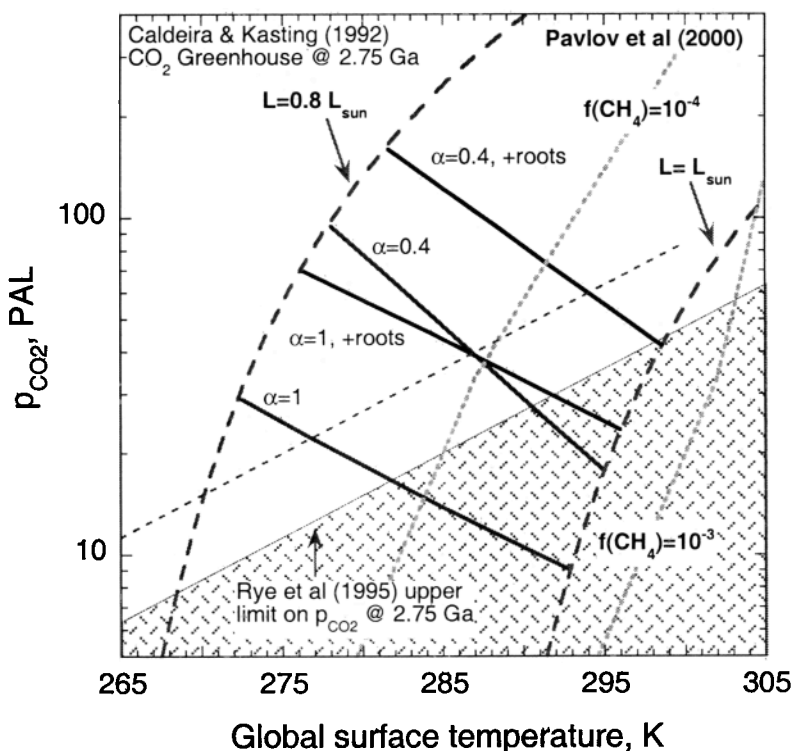
Figure 9. Atmospheric CO_2 levels plotted against global average surface temperature at a particular moment in Earth's history. The greenhouse curve for the nominal solar flux 2.75 Ga [*Caldeira and Kasting*, 1992] lies above the stability locus of siderite deduced by *Rye et al.* [1995]; these curves reproduce the argument made in the latter study. As *Rye et al.* [1995] point out, conditions for which siderite is absent in paleosols, as observed, cannot be obtained for this solar luminosity. Either the paleosols represent localities where temperatures were substantially hotter than the global average, or other greenhouse gases increased the effective solar luminosity. To illustrate the former, we have offset the temperature by 10 K to represent the observation that soil chemistry in temperate climates is biased toward warm days [*Ekart et al.*, 1999] (dotted line). To illustrate the latter, we show methane-CO_2 greenhouses, labeled by methane abundance, computed by *Pavlov et al.* [2000]. These also refer to solar luminosity 2.75 Ga. Finally, we show four loci of successful models for varying effective solar luminosity ($0 < \lambda < 1$) as described by (14) with $\alpha=1$ or $\alpha=0.4$, with and without a change in weathering efficiency brought on by the advent of vascular land plants.
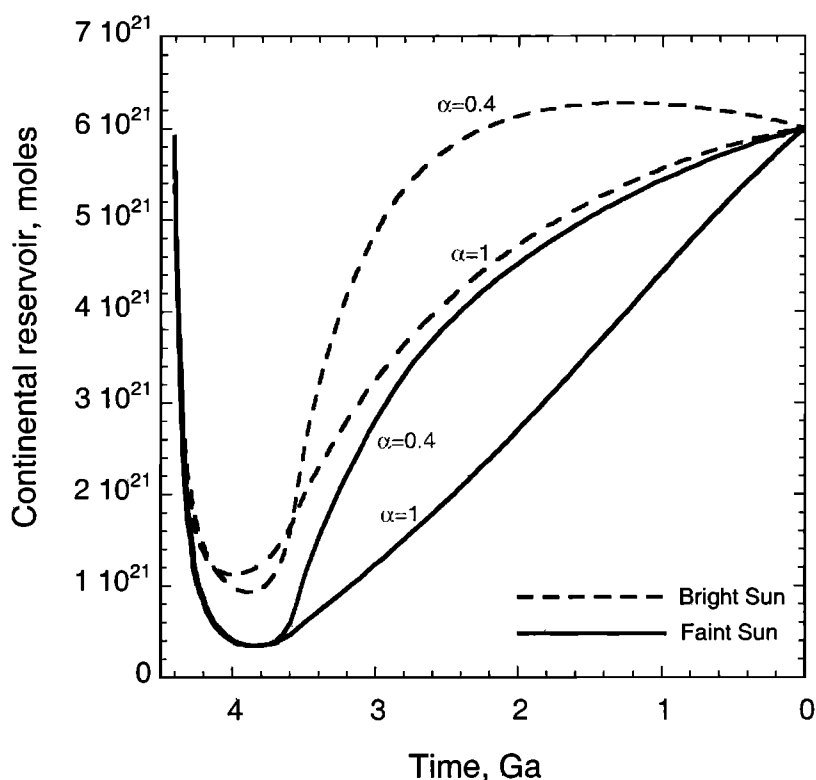
Figure 10. Continental reservoir size is computed as a function of time for $\alpha=1$ (dashed lines) and $\alpha=0.4$ (solid lines). A bright Sun results in earlier growth of the crustal reservoir. For $\alpha=0.4$ the crustal reservoir size reaches a maximum between 1 and 2 Ga and then decreases. These models include impact ejecta with $\gamma = 0.95$ in the Hadean.

the subtopics. (2) Other greenhouse gases may have been present, methane in particular. (3) The young Sun was less faint.

For these reasons and because available evidence indicates that the Archean Earth did not generally have an icehouse climate, we discuss the possibility that the Sun was less faint or that other greenhouse gases like methane were important [*Kiehl and Dickinson*, 1987; *Pavlov et al.*, 2000]. As the amount of such gases is not buffered by reactions with rocks in the manner of CO_2, we use the convenient method of treating both by modifying the solar luminosity. We use the arbitrary function

$$L = L_0\left(1 - 0.07\lambda t\right) \tag{14}$$

with $\lambda = 0.2$ rather than the standard $\lambda = 1$. The calculations are done for all of Earth history, even though it is obvious that high levels of methane cannot be maintained in an oxygen-rich atmosphere.

Computed temperature and carbon dioxide histories are shown in Figures 8a and 8b. As expected, a less faint Sun results in less atmospheric CO_2 and higher temperatures. The effect is significant even for $\alpha = 1$ where the hydrothermal sink is vigorous. The continental CO_2 reservoir grows faster with a brighter Sun as higher surface temperatures result in more silicate weathering and faster build up of carbonate on platforms (Figure 10). We conclude that even though a vigorous mantle cycle exists in the models, the Urey cycle including silicate weathering has significant effects, particularly in regulating the size of the crustal reservoir.

Return now to siderite. Figure 9 compares two families of our model predictions for global temperature and pCO_2 some 2.75 billion years ago to the local temperature and pCO_2 limits

obtained by *Rye et al.* [1995]. We generate model values of T and pCO_2 by presuming different solar luminosity histories $0 < \lambda < 1$ for our models with $\alpha = 0.4$ and $\alpha = 1$. Each model is constrained to evolve to $R_{con} = 6\times10^{21}$ mol and $pCO_2=3$ PAL at the present time; hence in these models both A_{hydro} and C_{SiO2w} vary as functions of λ. The standard faint sun ($\lambda = 1$) termini of the lines are defined by the *Caldeira and Kasting* [1992] curve. An Earth history with constant solar luminosity ($\lambda = 0$) is also marked. The portions of the lines below the siderite stability curve indicate conditions where siderite would be absent in paleosols formed at the mean global temperature. Again, the problem of whether the observed paleosols formed in regions hotter or colder than the global average arises. *Ekart et al.* [1999] argue that paleosols tend to record the warmest times of the year and that the typical overestimate for a temperate climate is ~10 K. We therefore show Rye et al.'s curve offset by 10 K. Doing so eliminates much of the perceived discrepancy.

3.1.4. Effect of the lack of land plants on the early Earth.

Land plants with roots have existed only since the Devonian period [e.g., *Berner*, 1997]. It might be expected that chemical weathering was sluggish before then [*Berner*, 1997]. We use this possibility to illustrate the general conclusion that a clement climate could have existed in the Archean if both silicate weathering and carbonation of oceanic crust were sluggish sinks requiring high pCO_2 to operate.

To quantify the effect of roots, we compute models based on the situation envisioned by *Berner* [1997]. Figure 11, the rooted analog to Figure 5, indicates what parameter values will lead to modern conditions. Our roots models differ from the rootless models by setting the weathering rate before the advent of 30% of
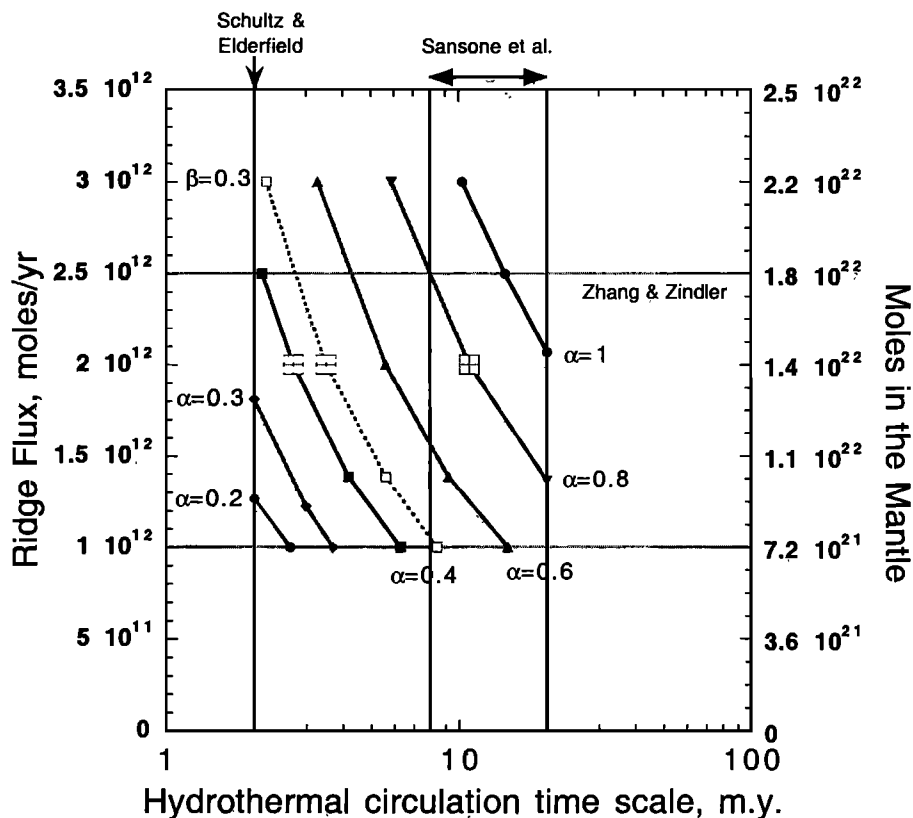
Figure 11. Loci of current parameter choices that can recreate the modern atmospheric and continental CO_2 inventories for models in which weathering changes with the advent of roots. These use $\beta = 0.5$ and reduce weathering rates before roots to 30% of what the rates are with roots. These values are consistent with *Berner* [1994, 1997]. For comparison we also show value used. The dotted line for $\beta = 0.3$, shows the effect of varying this parameter. The models indicated by large squares are presented in more detail in Figures 12 and 13.

the current rate, and for consistency with *Berner* [1994], we consider cases with $\beta = 0.5$ as well as $\beta = 0.3$. Particular models singled out for more attention are indicated on Figure 11, and these are presented in more detail in Figures 12a and 12b. These models use $\alpha = 0.8$ and a slow 16.3 m.y. cycle time and $\alpha = 0.4$ and a 2.7 m.y. cycle time (with $\beta = 0.3$ the cycle time is 3.5 m.y.). In all cases the lower silicate weathering rate over most of Earth's history means that allowable solutions require less seafloor carbonatization (see Figure 5). Sluggish weathering before the Devonian period results in higher pCO_2 (Figure 12a) and higher surface temperatures (Figure 12b), as expected. For $\alpha = 0.8$ the model is cold in the Archean because the flux of CO_2 into the oceanic crust acts as an effective buffer. Temperate conditions exist throughout the Archean with $\alpha = 0.4$. This model needs high pCO_2 because the oceanic crustal sink is relatively less important. Note, however, that the high pCO_2 levels in the root models conflicts with the *Rye et al.* [1995] evidence for the lack of siderite in paleosols (Figure 9).

3.2. Hadean Cycle and Impact Ejecta

The Hadean Era brought an additional threat to atmospheric CO_2. During the Hadean, impact ejecta would have been quantitatively important sediments [*Koster van Groos*, 1987]. Qualitatively, impact ejecta differ from other sediments in being pulverized, vitrified, or otherwise mechanically damaged and so relatively easily chemically attacked. Ejecta also tend to be more

mafic than more conventional sediments because the most frequent target is oceanic basalt and large impacts excavated material from the mantle. Like other oceanic sediments, weathered ejecta tended to be subducted along with the plates on which they are deposited. With more buffering by basic and ultrabasic rocks and with most of the weathering occurring at relatively low temperatures, the sink for CO_2 would have been greater, and the pH may have been higher [*Kempe and Degens*, 1985; *Kempe and Kazmierczak*, 1994]. Thus impact ejecta tended to draw down CO_2 more than the oceanic crust working alone, and the least CO_2 was left in the aftermath of the largest impacts. This effect is included in the models in Figures 6-11. We discuss our parameterization for ejecta in this section.

The flux of C in the impacting bodies can be safely ignored in the calculations. This can be seen most easily by noting that C is a small fraction of the impacting mass, and as shown in section 3.2.3, the amount of reactable ejecta is several times the impacting mass.

**3.2.1. The flux of impactors.** To quantify these effects, we begin with the impacting projectile that produced the ejecta. To first approximation the mass distributions of modern comets and asteroids appear to follow a power law of the form

$$N(> m) \approx (m/m_{max})^{-b}, \qquad (15)$$

where $N(> m)$ is the cumulative number of objects greater than mass m, m_{max} is the mass of the largest object in the distribution,
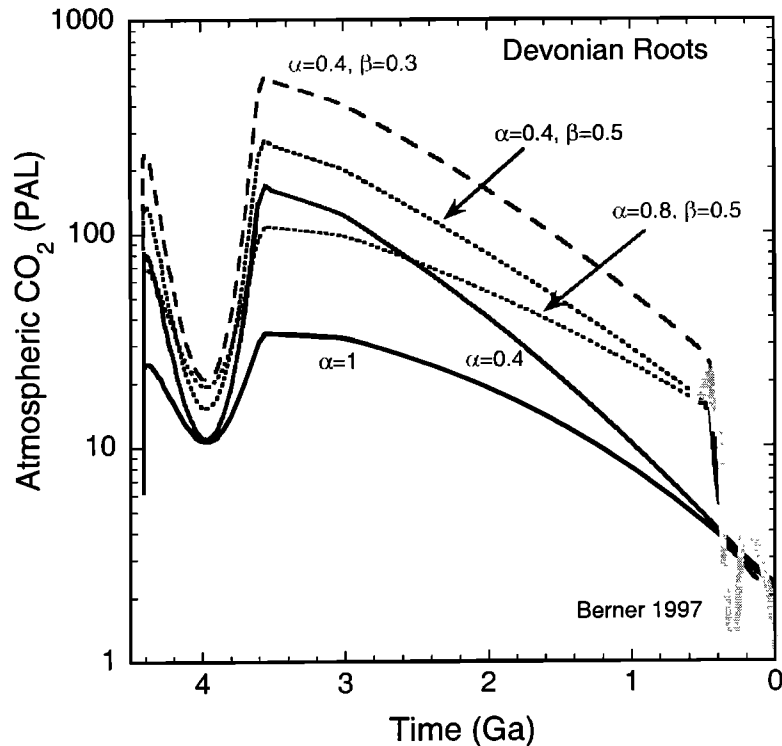
Figure 12a. Comparison of atmospheric CO_2 (pCO_2) histories for faint Sun models with and without a change in silicate weathering rates caused by roots. The solid lines indicate the standard models inidcated in Figure 5. The dashed lines denote the rooted models with $\beta = 0.5$, and the dotted line shows a rooted model with $\beta = 0.3$. Parameters for these three models are marked on Figure 11. Also shown for comparison is *Berner*'s [1997] pCO_2 curve.
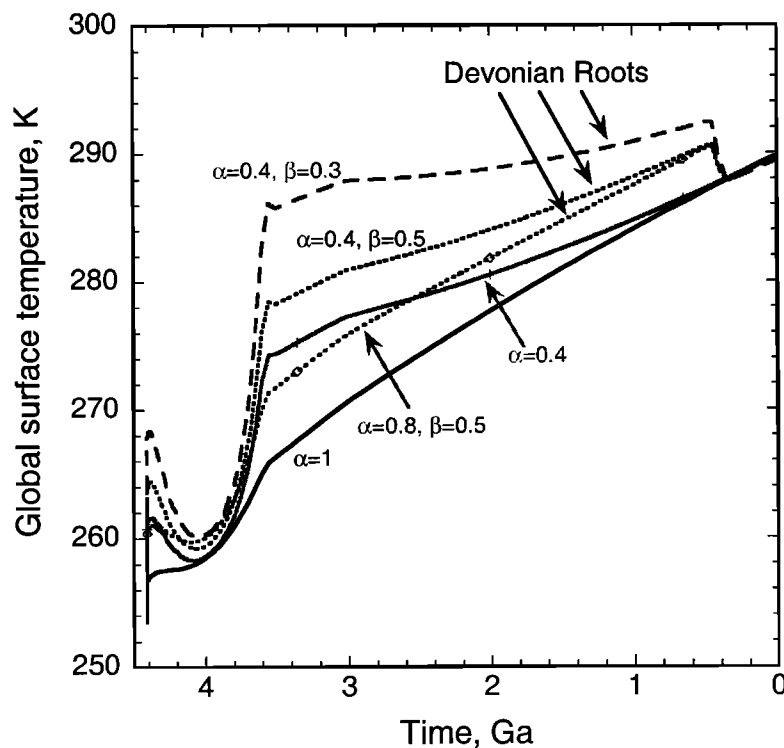
Figure 12b. Global surface temperature histories for the models in Figure 12a. By choosing favorable parameters ($\alpha = 0.4$, $\beta = 0.3$) we are able to construct a model that maintains a clement Earth (Figure 12b) using CO_2 alone through its post-Hadean history. Whether such models can be consistent with cold climates at the end of the Precambrian is something to consider.

and b is an exponent analogous to γ. Observed values of b are similar to that found theoretically to describe a fragmentation cascade, for which $b=5/6$ [Paolicchi, 1994; Williams and Wetherill, 1994]. The best choice of b for real solar system populations is debated and values as low as 0.5 and as high as 1.2 (for a finite part of the mass range) are seen in the literature; the best value probably lies between 2/3 and 5/6 [see Zahnle and Sleep, 1996; Anbar et al., 2001, and references therein]. Properties of power law distributions are discussed by Tremaine and Dones [1993]. An important property of the power law is that for $b<1$ the bulk of the mass is in the largest object or objects, which makes some predictions hostage to small number statistics at every scale over any period.

The Hadean ejecta production rate is best calibrated to the large lunar basins. These are large enough that many have been preserved and numerous enough (~30) that they are statistically well sampled. To order of magnitude the mass of the typical basin-forming impactor was $\sim 1 \times 10^{20}$ g, although the archetypes (Crisium, Imbrium, Nectaris, and Orientale) were larger ($\sim 1 \times 10^{21}$ g) and the largest one that remains, South Pole-Aitken, perhaps is $\sim 1 \times 10^{22}$ g. The last of the basins (Orientale, Imbrium, Schrödinger) formed ~3.85 billion years ago, so that to first approximation we can estimate an average lunar impact rate during the Hadean as a whole (~600 million years) to be ~3-10×10^{13} g yr^{-1}. At 3.9 Ga the accretion rate was still high, probably at least $\sim 1 \times 10^{13}$ g yr^{-1}.

To scale these rates to Earth requires that we take into account both Earth's greater target cross section and the length of the time interval τ we are looking at. Self-similarity of the power law (14) implies that the (median) total mass accreted by the Earth scales to that accreted by the Moon as [Anbar et al., 2001]

$$M_{i,E}(\tau) = M_{i,M}\left(\frac{A'_E \tau}{A'_M \tau_{\text{Had}}}\right)^{1/b}, \qquad (16)$$

where A'_E is the effective cross sectional area of the Earth, A'_M is the effective cross-sectional area of the Moon, and τ_{Had} is the duration of the Hadean Era. For typical asteroidal encounter velocities of ~15 km s^{-1} Earth's effective crosssection (including gravitational focusing) is ~20 times greater than the Moon's. For the Hadean as a whole we expect Earth to be struck by some 5-50×10^{23} g of material, at average rates of 1×10^{15}-1×10^{16} g yr^{-1}, depending rather strongly on the parameter b. However, most of this mass is in a few large impacts. The median value is less. For example, if we assume the same $\tau = 17$ million year crustal recycling time we assumed for the Archean, the expected median Hadean accretion rate on Earth is 2-20×10^{14} g yr^{-1}, while at 3.9 Ga we can take the median value to be $\sim 2 \times 10^{14}$ g yr^{-1}.

3.2.2. Reaction rates of basaltic glass. To affect the CO_2 cycle, the ejecta need to react before they are overturned into the mantle or buried below the depth of circulating fluids. We need to quantify this chemical process in order to model it.

Most ejecta fell into the ocean or were washed into the ocean and so weathered at low temperatures in the presence of water. For small impacts, all small ejecta were quickly quenched. For impacts large enough to form a transient rock vapor atmosphere, projectile diameter 70 km, ejecta falling on land may have welded into lava flows, but marine ejecta quenched when they hit the water. Marine ejecta may weld only if the ocean is boiled away. A colossal projectile >500 km diameter is needed to do that.

The quenched ejecta weathered like modern mafic and ultramafic volcanic glasses. Natural weathering of mafic glass to

form palagonite is fast in the modern ocean [Crovisier et al., 1987]. It is a direct sink for CO_2 in the mineral hydrotalcite $Mg_5Al_2CO_3(OH)_6 \cdot 4H_2O$. Natural weathering progresses with a linear rate of 2.6-4.3 mm m.y.$^{-1}$. That is, a 2.6-4.3 mm radius grain would weather to its center in a million years. Access of reactable seawater to the grain seems to be important in determining the kinetics as the Crovisier et al. [1987] laboratory rate is a factor of 40 higher.

Basaltic glass also dissolves readily on land if rainwater is available. Iceland provides a good example [Gislason and Arnórsson, 1993]. In regions where there is little biological activity, glass weathers rapidly enough that stream runoff is supersaturated in minerals, including olivine. The chemical weathering rate in these areas is 86 g m^{-2} r^{-2}. The composition of this chemical runoff is not given, but it is equivalent to a fraction, at least 0.5, of a mole of Ca^{2+} and Mg^{2+} per square meter per year. Extrapolating this cation flux to an Earth globally like Iceland gives a flux of 250×10^{12} mol yr^{-1}, which would, for example, when reacted with carbonate, remove the present crustal CO_2 reservoir in <30 m.y.

Marine basalt weathering is greatly enhanced by microbes both in the field [Thorseth et al., 1995] and the laboratory [Staudigel et al., 1995]. The Icelandic kinetics do depend on the CO_2 dissolved in the water and the acidity in general. Weathering is accelerated by a factor of 3 in regions that are acid either because of biological activity or volcanic gasses. However acid waters are not required. Weathering continues in waters isolated from the air to produce pH significantly greater than 9 [Gislason and Arnórsson, 1993].

In summary, it can be concluded that early Earth ejecta would have reacted with seawater and with rainwater when land existed. The reaction rates are fast even at temperatures close to the freezing point of water and are expected to be higher at temperate conditions [Brady and Gislason, 1997]. Yet reaction is not instantaneous. It takes hundreds of thousands of years to fully consume millimeter-size marine ejecta (a reasonable upper limit on the sizes of pulverized ejecta). The effect of ejecta or surface volcanics on ocean chemistry is averaged over this weathering time. Conversely, exposed lava and ejecta would have weathered extensively whenever the turnover time of the crust was greater than a few hundred thousand years.

3.2.3. Ejecta generation rate. We have two choices to compute the amount of reactable ejecta: (1) We can scale the volume of ejecta in proportion to the volume of the crater. This counts only the material that actually falls outside the crater. (2) We can scale the mass of reactable material to the volume of strongly shocked material. For large craters most of this "ejecta" does not actually leave the crater. For the first choice we scale the crater volume according to Schmidt and Housen [1987] to obtain

$$m_{ej} = 0.13 m_i (\rho_t/m_i)^{0.217} g^{-0.65} v_i^{1.3}, \qquad (17a)$$

where m_i is impactor mass, ρ_t is the density of the target, g is the acceleration of gravity, and v_i is the impactor velocity. For v_i=15 km s^{-1}, Earth gravity, and target density of 2.86 g cm^{-3}, the ejected mass in grams is

$$m_{ej} = 2.5 \times 10^{19} (m_i/10^{18})^{0.783} g, \qquad (17b)$$

where the impactor mass is in grams. For a 1×10^{21} g impactor,

$m_{ej} \sim 5.6 \ m_i$. For the second choice we can estimate the mass shocked to pressures $p > p_S$ by

$$m_s \approx m_i \left\{ Sv_i \Big/ c_B \left(\sqrt{1 + 4 S p_s / c_B^2 \rho_i} \ -1 \right) \right\}^{5/3} , \quad (18)$$

where c_B is the bulk sound velocity in the target and S is a dimensionless material constant. The shock pressure is approximated by

$$p_s = \rho_i v_s \frac{v_s - c_B}{S} , \quad (19)$$

where v_s is the shock velocity. For simplicity, we have assumed identical impactor and target materials. For basalt, $c_B = 2.6$ km s^{-1}, $S = 1.62$, and $\rho_i = 2.86$ g cm^{-3} [Melosh, 1989]. Rock shocked to pressures above the Hugoniot elastic limit, ~4.5 GPa, can be regarded as pulverized [Melosh, 1989]. Pulverization reduces the rock to debris of the order of the grain size. If we take pulverization as the activation threshold, at $v_i = 15$ km s^{-1} we obtain ~$17 m_i$ of reactable material per event. For dunite, perhaps a better analog to the target for large impacts, $c_B = 6.6$ km s^{-1}, $S = 0.9$, and $\rho = 3.32$ g cm^{-3}, the production rises to ~400 impactor masses. If we set the threshold higher, so that we require that the target reach the incipient melting threshold to be activated, we need to raise p_s to 44 GPa (dunite). There result ~$13 m_i$ of nearly melted dunite or ~$7 m_i$ of nearly melted basalt (not including the impactor itself). On the other hand, if we set the threshold lower, to include centimeter-size debris, impacts could generate thousands or even tens of thousands of impactor masses of reactable debris.

The two approaches, (17) and (18), are compatible for small impacts but not for large ones. Relatively little ejecta escape large craters, and some of this will be in large blocks. Meanwhile, much of the pulverized and melted material is deeply buried under the crater, where it may prove inaccessible to hydrothermal fluids.

The most conservative choice is to use the lesser of (17) and (18), which in practice, means choosing (17) and ignoring small impacts. The ejecta accumulation rate is then

$$\frac{\partial M}{\partial t} = \int \left(-\frac{\partial^2 N}{\partial t \partial m} \right) m_{ej}(m) \, dm = \frac{m_{max}^b}{\tau_{Had}} \int m_{ej}(m) m^{-1-b} \, dm . \quad (20)$$

The integral in (20) is not hard to evaluate for any b, but it takes on an especially simple form for $b = 0.783$. (Recall that we expect $0.6 < b < 0.9$ for plausible solar system populations). With this $b = 0.783$ we obtain the simple logarithmic result

$$\frac{\partial M}{\partial t} \approx \frac{m_{max}^b}{\tau_{Had}} \frac{25 \times 10^{18}}{\left(10^{18}\right)^{0.783}} \int m^{-1-b+0.783} \, dm$$

$$\approx \left(\frac{m_{max}}{10^{18}} \right)^{0.783} \frac{25 \times 10^{18}}{\tau_{Had}} \ln \left(\frac{m_{max}}{m_{min}} \right) , \quad (21)$$

which is 6×10^{15} g yr^{-1} for $m_{min} = 1 \times 10^{16}$ g and $m_{max} = 5 \times 10^{22}$ g. These refer to the smallest and largest impacts to generate significant ejecta. For an ocean-covered Earth, m_{min} is equivalent to the smallest impactor that can both penetrate the ocean and excavate unreacted basalt. The largest impact is estimated from the total mass accreted. We have approximated the relation between the total mass accreted M_{tot} and the largest mass in the distribution m_{max} by the median value [Anbar et al., 2001],

$$m_{max} \approx M_{tot} \left(1 - b^{1.4} \right) , \quad (22)$$

and we have taken in (21) $M_{tot} = 2 \times 10^{23}$ g and $\tau_{Had} = 300$ Ma as the duration of the late Hadean. The expected standing crop of basaltic and dunitic ejecta is 600 m from (21). In any event, our results are insensitive to m_{min}. Insensitivity to m_{max} and m_{min} applies for any likely value of b. However, there is a qualitative distinction between cases with $b < 0.783$ and $b > 0.783$. For $b < 0.783$, big impacts are more important sources of ejecta than small impacts, while for $b > 0.783$ the roles are reversed. The chief consequence of this is that climates driven by impacting populations with $b < 0.783$ fluctuate more wildly than climates driven by $b > 0.783$.

3.2.4. Ejecta reaction rate.

We now need to obtain the CO_2 sink associated with weathering of ejecta. One approach, albeit not conservative, is to assume that all or a constant fraction of the ejecta generated by an impact reacts quickly, in effect consuming all the CO_2 that it has cations for. We quantify this potential amount of reaction by assuming that reactable cations are present at 0.05 mol g^{-1}. This yields, from (21), an average flux of $F_{ej} = 3 \times 10^{14}$ moles yr^{-1}, a value that is less sensitive to the stochastics of small numbers than most other measures of impact. By this calculation, ejecta weathering would be so large that it cannot be balanced by the source terms in (7), and there is no steady state solution.

To this point, we have assumed that the flux of CO_2 is independent of pCO_2 and the reservoir size R_{oo}. However, ejecta can immediately remove only the accessible CO_2 in the atmosphere and the ocean. Over longer times, the ejecta flux is limited by the metamorphic, ridge, and arc sources on the right-hand side of (7). As these sources do not directly involve the impacts, the ocean plus atmosphere reservoir would be nearly exhausted if the available cation flux from ejecta exceeded the CO_2 sources in (7). In that case, pCO_2 would be reduced to a point that the time for degassed CO_2 to find ejecta with which to react mattered. This possibility is discussed in section 3.2.5. Note that over time, a large ejecta flux would strongly deplete crustal reservoirs of CO_2 as the CO_2 vented by metamorphism from the crust was cycled via ejecta to the mantle.

A second, relatively simple approach is to treat the ejecta as additional reactable oceanic crust. According to (21), the typical middle-to-late Hadean ejecta generation rate is ~6×10^{15} g yr^{-1}. New reactable oceanic crust was created at a rate of 5×10^{15} g yr^{-1}, assuming a global spreading rate of 10 times the present rate of 3 km^2 yr^{-1} and a reactable depth of 500 m. These numbers are comparable, but the damaged condition of the ejecta would make it more reactive than the basalt. By assumption the feedback would be of the same character as that for the oceanic crust alone, only stronger. With these assumptions it appears quite likely that reactions with ejecta will determine pCO_2.

A third, more ambitious, approach is to assume a mass distribution for the ejecta and directly estimate the corresponding weathering rate using the information given above. For the sake of specificity, let us describe the cumulative mass distribution by another power law $N(>\mu) \propto \mu^{-\gamma}$, where μ is the fragment mass. The character of the result depends almost entirely on the choice of γ. The effects are as described above: for $\gamma < 1$, weathering goes as $pCO_2^{3-3\gamma}$, whereas for $\gamma \geq 1$, weathering is nearly independent of pCO_2. Only for $\gamma < 1$ is there any significant negative feedback on pCO_2. That much (probably no less than 10%) of the K/T ejecta were smaller than millimeter-size implies that initially $\gamma > 0.95$; whether settling and compaction later lowered the effective value of γ is a fair question.

We estimate the reaction rate of ejecta by assuming that the mass-size distribution of the debris follows the $N(>\mu) \propto \mu^{-\gamma}$ power law and that individual particles are consumed at 3 mm per million years consistent with the data of *Crovisier et al.* [1987]. For $\gamma < 1$,

$$m_w = m_{ej} \frac{\int_0^{\mu_d} \mu^{-\gamma} d\mu + 3^{2/3} \int_{\mu_d}^{\mu_{max}} \mu^{-\gamma-1} d\mu}{\int_0^{\mu_{max}} \mu^{-\gamma} d\mu}$$

$$= m_{ej} \left(\frac{\mu_d}{\mu_{max}}\right)^{1-\gamma} \left(1 + \frac{3^{2/3}(1-\gamma)}{\gamma - 2/3}\right), \quad (23)$$

where we have defined $\mu_d = 4\pi\rho d^3$ to be the largest particle completely consumed at a time t and $d = 3$ mm pCO_2 $(t/10^6$ yr) to be the depth reacted $(\mu_d = 1.0$ g for $d=3$ mm, $t=1$ m.y., and $\rho = 3$ g cm^{-3}); μ_{max} refers here to the largest ejectum produced by the impact of mass m_i. We can take $\mu_{max}\sim0.01m_i$. If we assume that reactable cations are present at 0.05 moles/g, we obtain net CO_2 sinks following a single impact of

$$f_{ej}(\leq t) = \frac{1.25 \times 10^{18}}{10^{18(1-\gamma)}} \left(\frac{\mu_{max}}{m_i}\right)^{1-\gamma} \left(\frac{m_i}{10^{18}g}\right)^{\gamma - 0.217}$$

$$\bullet \left(1 + \frac{3^{2/3}(1-\gamma)}{(\gamma - 2/3)}\right) pCO_2^{3-3\gamma} t_6^{3-3\gamma},$$

$$= 3.0 \times 10^4 m_i^{0.683} pCO_2^{0.3} t_6^{0.3} \quad \text{mol} \quad \gamma = 0.9,$$

$$= 1.7 \times 10^4 m_i^{0.733} pCO_2^{0.15} t_6^{0.15} \quad \text{mol} \quad \gamma = 0.95, \quad (24a)$$

in which the notation t_6 refers to time measured in million year intervals. E.g., over an Archean oceanic crustal lifetime of 17 Ma, the ejecta with $\gamma = 0.95$ consume

$$f_{ej} \approx 4 \times 10^{17} \left(m_i / 10^{18} g\right)^{0.733} pCO_2^{0.15} \quad \text{mol} \quad (24b)$$

of CO_2. If we integrate (24a) over the distribution of impactors (15), we obtain

$$F_{ej} = \int_{m_{min}}^{m_{max}} f_{ej} \left(-\frac{\partial \tilde{N}}{\partial m}\right) dm, \quad (25a)$$

which for $\gamma = 0.9$, is

$$F_{ej} \approx \frac{bm_{max}^b}{\tau_{Had}} \frac{3.0 \times 10^4 t_6^{0.3}}{b - 0.683} \left(m_{min}^{0.683-b} - m_{max}^{0.683-b}\right) pCO_2^{0.3},$$

$$\approx 2 \times 10^{13} pCO_2^{0.3} \quad \text{mol yr}^{-1}, \quad (25b)$$

where we have evaluated terms for $b=0.783$, $t_6=17$, and $m_{min}=1\times10^{16}$ g. For $\gamma = 0.95$ and the same parameters the CO_2 flux is

$$F_{ej} \approx \frac{bm_{max}^b}{\tau_{Had}} \frac{1.7 \times 10^4 t_6^{0.15}}{b - 0.733} \left(m_{min}^{0.733-b} - m_{max}^{0.733-b}\right) pCO_2^{0.15},$$

$$\approx 8 \times 10^{13} pCO_2^{0.15} \quad \text{mol yr}^{-1}. \quad (25c)$$

Because these expressions are dominated by the smallest impactors, the quantity F_{ej} is not very jittery. If, instead, we take $\gamma = 1$, we obtain

$$f_{ej} = 1.0 \times 10^4 m_i^{0.783} \frac{\ln(\mu_d/\mu_{min}) + 3^{5/3}}{\ln(\mu_{max}/\mu_{min})}$$

$$\approx 7 \times 10^{17} \left(\frac{m_i}{10^{18}g}\right)^{0.783} \quad \text{mol}, \quad (26)$$

where the logarithms span some 40 orders of magnitude from $\mu_{max} = 0.01$ m_i to $\mu_{min} = 10^{-18}$ g (micron-sized grains). When f_{ej} is integrated over all m_i in (15) for $b=0.783$, another wide-spanning logarithm results:

$$F_{ej} = 5400 \frac{m_{max}^{0.783}}{\tau_{Had}} \ln\left(\frac{m_{max}}{m_{min}}\right) \approx 1.6 \times 10^{14} \text{mol yr}^{-1}, \quad (27)$$

which is, to within a factor 2, the same result we obtained at the beginning of this section for immediate and complete reaction of ejecta. This correspondence and the logarithmic or near-logarithmic dependencies in (25) and (27) imply that the median value of the flux F_{ej} is insensitive to the poorly constrained details of ejecta fragmentation and weathering.

It is necessary to make assumptions about the impactor flux to compute CO_2 histories for the early Earth. The timedependence of impactor flux is obtained from the lunar impact flux, which itself is controversial. Lunar flux estimates are, in part, extrapolations back in time from the better constrained flux around 3.8-3.9 Ga. For our purposes, it is not particularly important to choose sides in this debate. We have assumed a linear decline of the Hadean impact flux from an initially high value at 4.4 Ga to zero at 3.55 Ga, which yields a flux at 4.4 Ga at the lower end of estimates. More aggressive extrapolations, such as an exponential increase back in time, would imply greater impact flux, less atmospheric CO_2, and colder climates in the early Hadean than in our models.

The effective reactability of ejecta is represented by the parameter γ. For $\gamma > 1$ the model formulation predicts that there should be no CO_2 in the ocean or air. Actually, a finite amount should exist because of the finite circulation times of air and water. This situation is discussed in section 3.2.5.

The models in Figures in 6-11 assume $\gamma = 0.95$. To appraise the effect of this parameter, models with $\gamma = 0.9$ and no ejecta are computed (Figures 13a and 13b). All the models assume $b=0.783$. For the models with $\alpha = 0.3$, where the hydrothermal sink is sluggish, the presence of reactable ejecta greatly decreases pCO_2. The effect is more moderate for $\alpha = 1$, as this variant is already so cold in the Hadean that adding another sink on pCO_2 has only a modest effect.

From Figures 6-11, 13a, and 13b it is evident that reactable ejecta would have had a significant effect on the CO_2 cycle and on surface temperatures in the Hadean. It is evident from Figure 13 that the reactability of ejecta (here represented by γ) determines how significant the effect was.

3.2.5. Ejecta-dominated climate.

We have so far assumed in this paper that the mixing times of the oceanic and atmospheric reservoirs of CO_2 are too brief to affect the crustal and mantle cycles. The assumption that these reservoirs are in equilibrium is questionable when reactions involving ejecta greatly depleted them. The atmospheric CO_2 at such times would have been low but not zero because a finite time is needed for CO_2 degassed into the air to equilibrate with the ocean and for the oceanic CO_2 to come into contact with reactable rock. Climatic buffering at low surface temperatures is implied by both processes.

Geothermal heat alone would have prevented the ocean from freezing to the bottom [*Bada et al.*, 1994]. For example, an
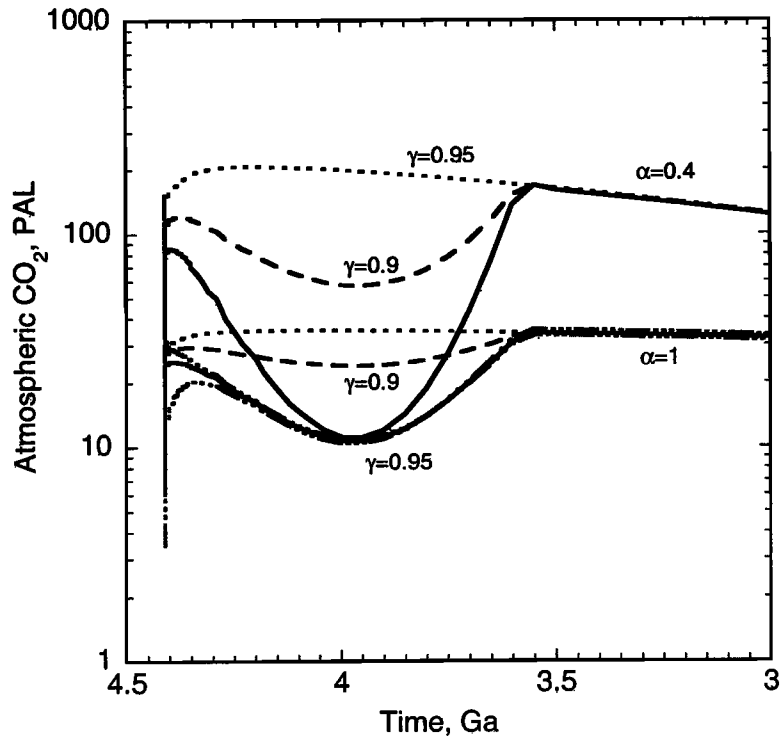
Figure 13a. The influence of different models of impact ejecta on the Hadean and early Archean CO_2 levels in our standard faint Sun models, for $\alpha=1$ and $\alpha=0.4$. We show three cases in which the reactability of ejecta to form carbonates ranges from none to a highly reactive case ($\gamma=0.95$); the intermediate case takes $\gamma=0.9$ ((23) and following). Reactable ejecta has strong effects for $\alpha=0.4$ and weaker effects for $\alpha=1$, where atmospheric CO_2 is already very low even without ejecta. A value of $\gamma>1$ (not shown) would reduce pCO_2 to zero in this model. In actuality, a small amount of CO_2 persists in even the most aggressive models owing to the finite mixing times of air and water.
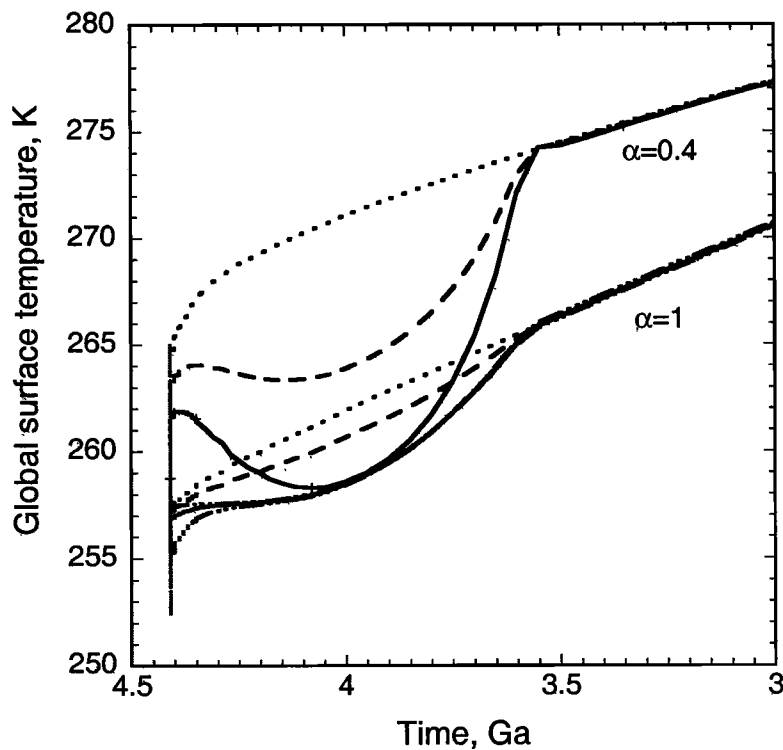
Figure 13b. The influence of different models of impact ejecta on the Hadean and early Archean surface temperature in our standard faint Sun models, for $\alpha=1$ and $\alpha=0.4$. Weathering of abundant ejecta produces very cold climates on the Hadean Earth unless greenhouse gases other than CO_2 were abundant.

average heat flow of 0.24 W m^{-2} (the average over the 17 m.y. lifetime of ocean crust in the nominal model) and a temperature difference of 20 K between the top and bottom of the ice imply an average ice thickness of 170 m for a conductivity of 2 W m^{-1} K^{-1}. The ice would be thinner near shores and over high heat flow regions. Wind ablation (which implies that as much water freezes at the base of the ice as sublimates from the surface, with the freezing water liberating its latent heat) and sunlight directly absorbed within or below the ice would reduce ice thickness still further, to as little as 10 m on average near the equator [*McKay*, 2000].

Ice movements likely produced lanes and leads wherever ice was thin. Lanes and leads in modern sea ice provide a useful analogy for the efficacy of gas exchange between sea and air as the process is efficient around the Antarctica ice when CO_2 disequilibrium exists [*Chen*, 1994].

How much CO_2 would actually be in the atmosphere of a mostly ice-covered Hadean Earth can be quantified by considering fluxes and residence times or, alternatively, by determining the area of open water needed to transfer the CO_2. The simpler approach is to estimate pCO_2 by multiplying the residence time by the effective volcanic flux into the atmosphere. We have estimated that the total outgassing flux of CO_2 (see Figure 7) was about 500×10^{12} mol yr^{-1} during the Hadean. However, only the CO_2 directly vented to the air could accumulate there because CO_2 vented into the ocean would have been quickly consumed by reactions with ejecta and basalt. On Earth today, ridges vent mainly into the ocean, while arcs vent mainly into the air. Here we assume that the Hadean was not fundamentally different in this regard, and so we assume that 50% of the total CO_2 flux was vented into the air. With this flux an atmospheric residence time of 220 years would be needed to maintain 1 PAL of CO_2, and a residence time of 0.7 m.y. would be needed to maintain 1 bar.

A different approach is to balance the effective outgassing flux against the flux of CO_2 that enters the ocean through open water. We begin with the hypothesis that air-sea exchange can be considered as diffusion across a thin surface film of ~30 µm above mixed seawater [*Broecker and Peng*, 1974]. The exchange rate is proportional to the disequilibrium in pCO_2 between the mixed sea and the air. For the numbers given by *Broecker and Peng* [1974] the flux of CO_2 per unit area is 4×10^3 mol m^{-2} yr^{-1} PAL^{-1}. An exposed sea surface area of 62,500 km^2 would suffice to maintain 1 PAL CO_2. This is comparable to the surface area of Lake Michigan. The area of open water must be reduced to no more than 20 km^2 worldwide to support 1 bar of CO_2.

We conclude that small but significant amounts of atmospheric CO_2 would have been present if direct venting to the air occurred and if ice cover impeded air-sea exchange. Air-sea exchange must be extremely sluggish with no open water for a thick CO_2 atmosphere to build up even with Hadean fluxes. The apparent brief existence of open water on Europa, where the surface temperature 100 K is far colder than any realistic surface temperature for the Earth, implies that total suppression of air-sea exchange by ice is unlikely on the early Earth .

Once mixed or erupted into the ocean, a finite time is required for water with dissolved CO_2 to find rock with which to react, provided that reaction with dissolved Ca^{2+} does not cause immediate removal. The oceanic circulation time for an ice-covered Earth is less than the circulation time obtained by considering only internal heat flow. For example, if the internal heat flow was 0.24 W m^{-2}, a 2.5 km thick column of water would be heated by 1 K in 2000 yr. This implies that a circulation time

longer that a few thousand years is unlikely as unstable temperature differences within the water column are highly unlikely to exceed a few Kelvin. An oceanic circulation time of 10^4 years and a Hadean flux 50×10^{12} mol yr^{-1} together imply a pool of 5×10^{18} mol of CO_2 in the ocean. For the present pH, one sixtieth of this amount is at equilibrium in the air, or 0.1×10^{18} mol, which is about 1.6 PAL. There is thus no obvious strong climatic buffer associated with the ocean circulation.

Climate buffering is implied by CO_2 exchange controlled by lanes. A warming climate implies thinner ice, more lanes, and hence more CO_2 leaving the air for the ocean. This flux cools the climate and thickens the ice. Conversely, a cooling climate produces thicker ice and fewer leads, favoring the accumulation of CO_2 in the air.

During the Hadean, another dynamic climate buffer is implied by the interaction of dust and snow. Consider a cold, fully ice-covered Earth. Little vaporization would occur, and there would be little moisture to fall as snow. Surface ice would have become covered with dust from volcanoes and ejecta. Land areas (if any existed) would be exposed in areas of net ice sublimation; these too would contribute windblown dust to the icecaps. The dust lowers the albedo and warms the climate. Conversely, a warmer climate precipitates more snow, covering the dust, increasing the albedo, and cooling the climate. A similar buffer operates within the ablation zones on sea ice. Here snow removal creates black ice, which has a much lower albedo than snow.

Note that a dust albedo buffer depends on the global area covered by surface lag deposits within ablation zones at sea and on land, increasing as open water and snowfall decrease. The buffer does not involve dust globally overwhelming snowfall. The global rate of ablation and hence snowfall is quite large even for a cool Earth [*McKay*, 2000]. As a case colder than any reasonable Hadean Earth, Mars at the present has a surface temperature of -60°C and a calculated ablation rate of 1-2 cm yr^{-1} [*Squyres*, 1989]. These rates far exceed any global long-term average rate of sediment or ejecta accumulation. A dust accumulation at this rate could occur only transiently after individual impacts and locally near eruptions and windswept outwash plains.

Overall, we expect a cold Earth to hover about a stable buffer that is warm enough to produce some fresh snow but dry enough that significant areas are free of high-albedo snow and ice. The sea lanes couple this buffer to the air-sea exchange buffer for CO_2 discussed above. A drastic pCO_2 disequilibrium was precluded by open lanes at this and any subsequent time.

4. Conclusions and Biological Implications

We have investigated the CO_2 cycle on the early Earth using the modern Earth as an analog. The traditional crustal reservoir of platform carbonates grows when silicate weathering supplies cations and shrinks when metamorphism liberates CO_2 while stranding the cations at depth. Over long timescales the mantle reservoir exchanges CO_2 with the crustal reservoir. Even today, significant fluxes from the mantle occur at mid ocean ridge axes and island arcs. Subduction of carbonatized oceanic basalt and, in recent times, pelagic carbonate return crustal CO_2 to the mantle. The oceanic crust, the ocean, and the atmosphere are small reservoirs that act to transfer CO_2 within the crust and between the crust and the mantle.

It is well known that the crustal Urey cycles of silicate weathering and metamorphism function as a dynamic buffer for atmospheric pCO_2 and climate. Yet it appears that the present

CO_2 abundance in the ocean and atmosphere is in part dynamically maintained by cycles involving the mantle. Feedback is provided by the dependence of the amount of carbonatization of oceanic crust on pCO_2. Early in the Earth's history, vigorous mantle cycles may have been dominant. A massive CO_2 greenhouse is precluded, and globally freezing temperatures indicated freezing temperature occurred unless another greenhouse gas was important. Conversely, traditional representations of the Hadean CO_2 cycle which do not include significant ejecta and basalt sinks result in massive warm Hadean CO_2 atmospheres [Morse and Mackenzie, 1998].

In our model the oceanic crust acts as the subductable carbonate trap that closes the mantle CO_2 cycle. Factors that inhibit carbonate subduction have the effect of stranding CO_2 in surface reservoirs. Perhaps the most important caveat is that although the capacity of the oceanic basalt reservoir CO_2 is large ($\sim 3\times10^{21}$ mol), it can accommodate only a fraction of the global inventory of 25×10^{21} mol of CO_2. The possibility thus arises that the buffer imposed by carbonitization of the oceanic crust could have been overwhelmed early in the Earth's history if CO_2 in subducted crust was nearly quantitatively degassed back to the surface at island arcs. Our models indicate that this occurs when C_{deep}, the fraction of subducted carbonate that reaches the mantle, becomes smaller than 20%. This is much smaller than the modern value of 64-84% [Fischer et al., 1998]. A massive CO_2 atmosphere could result if $C_{deep} < 0.2$. We do not examine whether this actually occurred on the Earth or how long it lasted. We do note that surface temperatures of over 200°C are implied [Kasting and Ackerman, 1986]. The Earth would not have been habitable until C_{deep} became large enough that mantle fluxes to the surface could be balanced by subduction fluxes to the deep interior. Thereafter, the more benign climates implied by our models would have prevailed.

The Hadean differed from the rest of the Earth's history in that reactable ejecta provided an effective CO_2 sink. The reactability of ejecta determines how low pCO_2 and surface temperature go. All our models predict cold surface temperatures in the Hadean. The Earth surface would have been cold and the ocean ice covered if another greenhouse gas was not important. Under such circumstances, small amounts of atmospheric CO_2 were dynamically maintained by the finite time for degassed CO_2 to get into the ocean.

The existence of massive deposits of reactive impact ejecta implies relatively low CO_2 levels in the Hadean atmosphere. This has implications to the origin of life in that modest amounts of degassed CH_4 and CO might have built up to levels comparable to or greater than that of CO_2. These and other reduced gases (e.g., H_2) wouldld have also been produced in significant episodic quantities by the reaction of metallic iron supplied by impacting bodies and with surface water and CO_2 [Kasting, 1990]. High atmospheric ratios of CH_4/CO_2 favor formation of complex reduced carbon compounds by abiogenic processes [e.g., Zahnle, 1986; McKay et al., 1997]. An ice-covered Earth has itself been recommended as an environment for the origin of life [Bada et al., 1994].

References

Abbott, D. L., L. Burgess, J. Longhi, and W. H. F. Smith, An empirical thermal history of the Earth's upper mantle, J. Geophys Res., 99, 13,835-13,850, 1994

Allard, P., P. Jean-Baptiste, W. D'Alessandro, F. Parello, B. Parisi, and C. Flehoc, Mantle-derived helium and carbon in ground waters and gases of Mount Etna, Italy, Earth Planet. Sci. Lett., 148, 501-516, 1997.

Alt, J. C, Low temperature alteration of basalts from the Hawaiian ridge, Leg 136, Proc. Ocean Drill. Program Sci Results, 136, 133-146, 1993.

Alt, J. C., Subsurface processes in mid-ocean ridge hydrothermal systems, in Seafloor Hydrothermal Systems, Physical, Chemical, Biological, and Geological Interactions, Geophys. Monogr. Ser, vol. 91, edited by S. E. Humphris et al., pp. 85-114, AGU., Washington, D. C , 1995

Alt, J. C., and D. A. H. Teagle, The uptake of carbon during alteration of oceanic crust, Geochim. Cosmochim. Acta, 63, 1527-1535, 1999.

Alt, J. C., K. Muehlenbachs, and J. Honnorez, An oxygen isotope profile through the upper kilometer of the oceanic crust, DSDP Hole 504B, Earth Planet. Sci. Lett., 80, 217-229, 1986.

Alt, J. C., D. A H. Teagle, C. Laverne, D. A. Vanko, W. Bach, J. Honnorez, K. Becker, M. Ayadi, and P. A. Pezard, Ridge flank alteration of upper ocean crust in the eastern Pacific: Synthesis of results for volcanic rocks of Holes 504B and 896A, Proc. Ocean Drill. Program Sci. Results, 148, 435-450, 1996a.

Alt, J. C., et al., Hydrothermal alteration of a section of upper oceanic crust in the eastern equatorial Pacific: A synthesis of the results from Site 504 (DSDP Legs 69, 70, and 83 and ODP legs 111,137, 140, and 148), Proc. Ocean Drill Program Sci Results, 148, 417-434, 1996b.

Anbar, A. D., G. L. Arnold, S. J. Mojzsis, and K. J. Zahnle, Extraterrestrial iridium, sediment accumulation and the habitability of the early Earth's surface, J. Geophys. Res., in press, 2001.

Bada, J. L., C. Bigham, and S. L. Miller, Impact melting of frozen oceans on the early Earth implications for the origin of life, Proc. Natl. Acad. Sci. U. S. A, 91, 1248-1250, 1994.

Berner, R. A., A model for atmospheric CO_2 over Phanerozoic time, Am. J. Sci., 291, 339-376, 1991.

Berner, R. A., 3GEOCARB II: A revised model of atmospheric CO_2 over Phanerozoic time, Am. J. Sci., 294, 56-91, 1994.

Berner, R. A., The rise of plants and their effect on weathering and atmospheric CO_2, Science, 276, 544-546, 1997

Brady, P. V., and S. R. Gíslason, Seafloor weathering controls on atmospheric CO_2 and global climate, Geochim. Cosmochim. Acta, 61, 965-973, 1997.

Brantley, S. L., and K. W. Koepenick, Measured carbon dioxide emissions from Oldoiyo Lengai and the skewed distribution of passive volcanic fluxes, Geology, 23, 933-936, 1995.

Broecker, W. S., and T.-H. Peng, Gas exchange rates between air and sea, Tellus, 226, 21-35, 1974.

Buick, R., and J. S. R. Dunlop, Evaporitic sediments of early Archean age from the Warrawoona Group, North Pole, Western Australia, Sedimentology, 37, 247-277, 1990.

Caldeira, K., Long term control of atmospheric carbon· Low-temperature seafloor alteration or terrestrial silicate-rock weathering?, Am J. Sci., 295, 1077-1114, 1995.

Caldeira, K., and J. F. Kasting, The life span of the biosphere revisited, Nature, 360, 721-723, 1992.

Carlson, R L., Seismic velocities in the uppermost oceanic cust: Age dependence and the fate of layer 2A, J. Geophys. Res, 103, 7069-7077, 1998.

Chen, C.-T. A , Some indications of excess CO_2 penetration near Cape Adare off the Ross Sea, La mer, Bull Soc. Fr. Jp. Oceanogr., 32, 167-172, 1994.

Crovisier, J. L., J. Honnorez, and J. P. Eberhart, Dissolution of basaltic glass in seawater· Mechanism and rate, Geochim. Cosmochim. Acta, 51, 2977-2990, 1987.

Des Marais, D J., and J. G Moore, Carbon and its isotopes in mid-oceanic basaltic glasses, Earth Planet. Sci. Lett., 69, 43-57, 1984.

deWit, M. J., and R. A. Hart, Earth's earliest continental lithosphere, hydrothermal flux and crustal recycling, Lithos, 30, 309-335, 1993.

Donnelly, T., J. Francheteau, W. Bryan, P. T. Robinson, M. F. J. Flower, and M. Salisbury, Initial Reports of Deep Sea Drilling Prog., vol. 51-53, U.S. Gov. Print. Off, Washington, D. C , 1979.

Ekart, D D , T. E. Cerling, I. P. Montañez, and N. J. Tabor. A 400 million year carbon isotopic record of pedogenic carbonate· Implications for paleoatmospheric carbon dioxide, Am. J. Sci., 299, 805-827, 1999.

Fischer, T. P., W. F Giggenbach, Y Sano, and S. N Williams, Fluxes

and source of volatiles dischanged from Kudryavy, a subduction zone volcano, Kurile Islands, *Earth Planet. Sci. Lett., 160*, 81-96, 1998.

Fisher, A. T., Permeability within basaltic oceanic crust, *Rev. Geophys., 36*, 143-182, 1998.

Franck, S., K. Kossacki, and C. Bounama, Modelling the global carbon cycle for the past and future evolution of the earth system, *Chem. Geol., 159*, 305-317, 1999.

François, L. M., and Y. Goddéris, Isotopic constraints on the Cenozoic evolution of the carbon cycles, *Chem. Geol., 145*, 177-212, 1998.

François, L. M., and J. C. G. Walker, Modelling the Phanerozoic carbon cycle and climate: Constraints from the $^{87}Sr/^{86}Sr$ isotopic ratio of seawater, *Am. J. Sci., 292*, 81-135, 1992.

Garrels, R. M., and F T Mackenzie, *The Evolution of Sedimentary Rocks*, 397 pp., Norton, New York, 1971.

Gerlach, T. M., Present-day CO_2 emissions from volcanoes, *Eos Trans. AGU, 72*, 249, 254-255, 1991.

Gíslason, S. R., and S. Arnórsson, Dissolution of primary basaltic minerals in natural waters: Saturation state and kinetics, *Chem. Geol., 105*, 117-135, 1993.

Goddéris, Y., and L. M François, The Cenozoic evolution of the strontium and carbon cycles: Relative importance of continental erosion and mantle exchanging, *Chem. Geol., 126*, 167-190, 1995.

Grotzinger, J. P., and J. F. Kasting, New constraints on Precambrian ocean composition, *J. Geol., 101*, 235-243, 1993.

Hoffman, P. E., and D. P. Schrag, Snowball Earth, *Scientific American, 282*(1), 50-57. 2000.

Holland, H. D., *The Chemistry of the Atmosphere and Oceans*, 351 pp., John Wiley, New York, 1978.

Holland, H. D., *The Chemical Evolution of the Atmosphere and Ocean*, 582 pp., Princeton Univ. Press, Princeton, N. J , 1984.

Hooft, E. E. E , H. Schouten, and R. S. Detrick, Constraining crustal emplacement processes from the variation in sesimic layer 2A thickness at the East Pacific Rise, *Earth Planet. Sci. Lett., 142*, 289-309, 1996.

Huang, W -L., P. J. Wyllie, and C. E. Nehru, Subsolidus and liquidus phase relationships in the system $CaO-SiO_2-CO_2$ to 30 kbar with geological applications, *Am. Mineral., 65*, 285-301, 1980.

Kadko, D., J. Baross, and J. Alt, The magnitude and global implications of hydrothermal flux, in *Seafloor Hydrothermal Systems, Physical, Chemical, Biological, and Geological Interactions, Geophys. Monogr. Ser.*, vol. 91, edited by S. E. Humphris et al., pp. 446-466, AGU, Washington, D. C., 1995.

Kasting, J. F., Bolide impacts and the oxidation state of carbon in the Earth's early atmosphere, *Origin Life Evol Biosphere, 20*, 199-231, 1990.

Kasting, J. F., Earth's early atmosphere, *Science, 259*, 920-926, 1993.

Kasting, J F., and T. P. Ackerman, Climatic consequence of very high carbon dioxide levels in the early Earth's atmosphere, *Science, 234*, 1383-1385, 1986.

Kempe, S., and E. T. Degens, An early soda ocean?, *Chem. Geol., 53*, 95-108, 1985.

Kempe, S., and J. Kazmierczak, The role of alkalinity in the evolution of ocean chemistry, organization of living systems, and biocalcification processes, *Bull. Inst. Oceanogr. Monoco, 13*, 61-117, 1994

Kiehl, J. T., and R. E. Dickinson, A study of the radiative effects of enhanced atmospheric CO_2 and CH_4 on early Earth surface temperatures, *J. Geophys. Res., 92*, 2991-2998, 1987.

Koster van Groos, A. F., Weathering, the carbon cycle, and differentiation of the continental crust and mantle, *J Geophys. Res., 93*, 8952-8958, 1988.

Langmuir, C. H., E. M. Klein, and T. Plank, Petrological systematics of mid-ocean ridge basalts: Constraints on melt generation beneath ridges, in *Mantle Flow and Melt Generation of Mid-ocean Ridges, Geophys. Monogr. Ser.*, vol. 71, edited by J. Phipps Morgan, D. K. Blackman, and J M Sinton, pp. 183-280, AGU, Washington, D. C., 1992.

Lasaga, A. C., R. A. Berner, and R. M Garrels, An improved geochemical model of atmospheric CO fluctuations over the past 100 million years, in *The Carbon Cycle and Atmospheric CO₂: Natural Variations Archean to Present, Geophys. Monogr. Ser.*, vol. 32, edited by E. T. Sundquist and W S Broecker, pp. 397-411, AGU, Washington, D. C., 1985.

Lowe, D. R., Petrology and sedimentology of cherts and related silicified sedimentary rocks in the Swaziland supergroup, in *Geologic Evolution of the Barberton Greenstone Belt, South Africa*, edited by D. R. Lowe and G. R. Byerly, pp 83-114, Geol. Soc. of Am., Boulder, Colo., 1999.

Macloed, G., C. McKeown, A. J. Hall, and M. J. Russell, Hydrothermal and ocean pH conditions of possible origin of life, *Origins Life Evol. Biosphere, 24*, 19-41, 1994.

Marty, B., and A. Jambon, C/He in volatile fluxes from the solid Earth: Implications for carbon geodynamics, *Earth Planet. Sci. Lett., 83*, 16-26, 1987.

Marty, B., and I. N. Tolstikhin, CO_2 fluxes from mid-oceanic ridges, arcs, and plumes. *Chem. Geol., 145*, 233-248, 1998.

McKay, C. P, Thickness of tropical ice and photosynthesis on a snowball Earth, *Geophys. Res. Lett., 27*, 2153-2156, 2000.

McKay, C. P., W. Borucki, and J. William, Organic synthesis in experimental impact shocks, *Science, 276*, 390-392, 1997.

Melosh, H. J., *Impact Cratering: A Geological Process*, Oxford Univ. Press, New York, 1989.

Michaud, V., Crustal xenoliths in recent hawaiites from Mount Etna, Italy: Evidence for alkali exchanges during magma-wall rock interaction, *Chem. Geol., 122*, 21-42, 1995.

Morse, J. W., and F. T. Mackenzie, Hadean ocean carbonate geochemistry, *Aquat. Geoch., 4*, 301-319, 1998.

Mottl, M. J., and C. C. Wheat, Hydrothermal circulation through mid-ocean flanks: Fluxes of heat and magnesium, *Geochim. Cosmochim. Acta, 58*, 2225-2239, 1994.

Nisbet, E. U., M. J. Cheadle, N. T. Arndt, and M. J. Bickle, Constraining the potential temperature of the Archaean mantle: A review of the evidence from komatiites, *Lithos, 30*, 291-307, 1993

Nutman, A. P., V. R. McGregor, C. R. L. Friend, V. C. Bennett, and P. D. Kinney, The Itsaq gneiss complex of southern West Greenland: The world's most extensive record of early crustal evolution (3900-3600 Ma), *Precambrian Res., 78*, 1-39, 1996.

Owen, T., R. D. Cess, and V. Ramanathan, Enhanced CO_2 greenhouse to compensate for reduced solar luminosity on early Earth, *Nature 277*, 640-642, 1979.

Paolicchi, P., Rushing to equilibrium: A simple model for the collisional evolution of asteroids, *Planet. Space Sci., 42*, 207-221, 1994.

Pavlov, A. A., J. F Kasting, L. L. Brown, K. A. Rages, and R. Freedman, Greenhouse warming by CH_4 in the Atmosphere of Early Earth, *J. Geophys. Res., 105*, 11,981-11,990, 2000.

Peacock, S. M., Thermal and petrologic structure of subduction zones, in *Subduction Top to Bottom, Geophys. Monogr. Ser*, vol. 96, edited by G. E. Bebout, D. W. Scholl, S. H. Kirby, and J. P. Platt, pp. 119-133, AGU Washington, D. C., 1996.

Peacock, S. M., T. Rusher, and A. B Thompson, Partial melting of subducting oceanic crust, *Earth Planet. Sci. Lett., 121*, 227, 244, 1994.

Phipps Morgan, J , Thermal and rare gas evolution of the mantle, *Chem. Geol , 145*, 431-445, 1998.

Plank, T., and C. H Langmuir, The chemical composition of subducting sediment and its consequences for the crust and mantle, *Chem Geol., 145*, 325-394, 1998.

Ringwood, A. E., Changes in solar luminosity and some possible terrestrial consequences, *Geochim. Cosmochim. Acta, 21*, 295-296, 1961.

Russell, M. J., and A. J. Hall, The emergence of life from iron monosulphide bubbles at a submarine hydrothermal redox and pH front, *J. Geol. Soc. London, 154*, 377-402, 1997.

Rye, R , P. H. Kuo, and H. D. Holland, Atmospheric carbon dioxide concentrations before 2.2 billion years ago, *Nature, 378*, 603-605, 1995.

Sagan, C., and G. Mullen, Earth and Mars. Evolution of atmospheres and surface temperatures, *Science, 177*, 52-56, 1972

Sano, Y., and S. N. Williams, Fluxes of mantle and subducted carbon along convergent plate boundaries, *Geophys. Res. Lett., 23*, 2749-2752, 1996.

Sansone, F. J., M. J. Mottl, E. J. Olson, C. G. Wheat, and M. D. Lilley, CO_2-depleted fluids from mid-ocean ridge-flank hydrothermal springs, *Geochim. Cosmochim. Acta, 62*, 2247-2252, 1998.

Schmidt, R. M., and K. R. Housen, Some recent advances in the scaling of impact and explosion cratering, *Int. J. Impact Mech., 5*, 543-560, 1987.

Schultz, A., and H. Elderfield, Controls on the physics and chemistry of seafloor hydrothermal circulation, *Philos. Trans. R. Soc. London, Ser. A., 355*, 387-425, 1997.

Schultz, A., and H. Elderfield, Controls on the physics and chemistry of seafloor hydrothemal circulation, in *Mid-ocean Ridges, Dynamics of Processes Associated with Creation of New Oceanic Crust*, edited by J. R. Cann, H. Elderfield, and A. Laughton, pp. 171-209, Cambridge Univ Press, New York, 1999.

Sibley, D. F., and T. A. Vogel, Chemical mass balance of the Earth's

crust. The calcium dilemma (?) and the role of pelagic sediments, *Science, 192,* 551-553, 1976

Sleep, N. H., Thermal history and degassing of the Earth: Some simple calculations, *J. Geol., 87,* 671-686, 1979.

Squyres, S. W , Urey Prize Lecture: Water on Mars, *Icarus, 79,* 229-288, 1989

Staudigel, H , S. R. Hart, H.-U Schmincke, and B. M. Smith, Cretaceous ocean crust at DSDP sites 417 and 418: Carbon uptake from weathering versus loss by magmatic outgassing, *Geochim. Cosmochim. Acta, 53,* 3091-3094, 1989.

Staudigel, H., R. A Chastain, A. Yayanos, and W. Bourcier, Biologically mediated dissolution of glass, *Chem. Geol., 126,* 147-154, 1995.

Staudigel, H , T. Plank, B. White, and H-U. Schmincke, Geochemical fluxes during seafloor alteration of basaltic upper oceanic crust: DSDP sites 417 and 418, in *Subduction Top to Bottom, Geophys. Monogr. Ser ,* vol 96, edited by G. E. Bebout et al., pp. 19-36, AGU, Washington, D C., 1996.

Stein, C. A., S. Stein, and A M. Pelayo, Heat flow and hydrothermal circulation, in *Seafloor Hydrothermal Systems, Physical, Chemical, Biological, and Geological Interactions, Geophys Monogr. Ser.,* vol. 91, edited by S. E. Humphris et al., pp. 425-445, AGU, Washington, D. C., 1995.

Stolper, E., and S. Newman, The role of water in the petrogenesis of Mariana trough magmas, *Earth Planet. Sci. Lett , 121,* 293-325, 1994.

Tajika, E , and T. Matsui, Evolution of terrestrial proto-CO_2 atmosphere coupled with thermal history of the Earth, *Earth Planet. Sci. Lett., 113,* 251-266, 1992.

Tajika, E., and T Matsui, Evolution of seafloor spreading rate based on [40]Ar degassing history, *Geophys. Res. Lett., 20,* 851-854, 1993.

Thorseth, I H , T Torsvik, H Furnes, and K. Muehlenbachs, Microbes play an important role in the alternation of oceanic crust, *Chem. Geol., 126,* 137-146, 1995.

Torgensen, T., Terrestrial helium degassing fluxes and the atmospheric helium budget: Implication with respect to the degassing processes of continental crust, *Chem. Geol., 74,* 1-14, 1989.

Tremaine, S., and L. Dones, On the satistical distribution of massive impactors, *Icarus, 106,* 335-341, 1993.

Walker, J. C G., *Evolution of the Atmosphere,* 318 pp., Macmillan, New York, 1977.

Walker, J. C G., Carbon dioxide on the early Earth, *Origins Life Evol. Biosphere, 16,* 117-127, 1985.

Walker, J. C G., P B. Hays, and J. F. Kasting, A negative feedback mechanism for the long-term stabilization of the Earth's surface temperature, *J. Geophys. Res., 86,* 9776-9782, 1981.

Williams, D A , and G. W. Wetherill, Size distribution of collisionally evolved asteroid populations. Analytical solution for self-similar collision cascades, *Icarus, 107,* 117-128, 1994.

Williams, D. R., and V. Pan, Internally heated mantle convection and thermal and degassing history of the Earth, *J Geophys. Res., 97,* 8937-8950, 1992.

Wolery, T J., and N. H. Sleep, Interactions of geochemical cycles with the mantle, in *Chemical Cycles in the Evolution of the Earth,* edited by C. B. Gregor et al., pp. 77-103, John Wiley, New York, 1988.

Zahnle, K., Photochemistry of methane and the formation of hydrocyanic acid (HCN) in the Earth's early atmosphere, *J. Geophys Res. 91,* 2819-2834, 1986.

Zahnle, K. and N. H Sleep, Impacts and the early evolution of life, in *Comets and the Origin and Evolution of Life,* edited by P. J. Thomas, C. F Chyba, and C. P. McKay, pp. 175-208, Springer-Verlag, New York, 1996.

Zhang, Y., and A. Zindler, Distribution and evolution of carbon and nitrogen in Earth, *Earth Planet. Sci. Lett., 117,* 331-345, 1993.

N. H. Sleep, Department of Geophysics, Stanford University, Mitchell Building, Room 360, 397 Panama Mall, Stanford, CA 94305. (norm@pangea.stanford.edu)

K. Zahnle, NASA Ames Research Center, Mountain View, CA 94035.